MODELING AND OPTIMIZATION OF RISER TYPE INDUSTRIAL FLUID CATALYTIC CRACKING UNIT

A DISSERTATION

Submitted in partial fulfillment of the requirements for the award of the degree of

MASTER OF TECHNOLOGY

in

CHEMICAL ENGINEERING

(With Specialization in Computer Aided Process Plant Design)

By

RAGHVENDRA SINGH

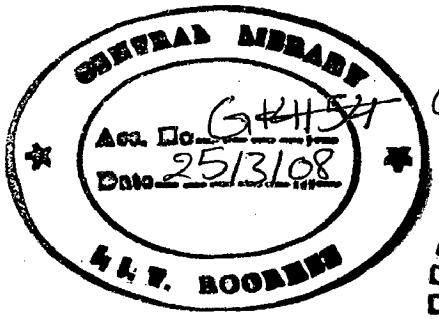

DEPARTMENT OF CHEMICAL ENGINEERING
INDIAN INSTITUTE OF TECHNOLOGY ROORKEE
ROORKEE - 247 667 (INDIA)
JUNE, 2007

INDIAN INSTITUTE OF TECHNOLOGY ROORKEE

ROORKEE

CANDIDATE'S DECLARATION

I declare that the work, which is being presented in the dissertation entitled **"MODELING AND OPTIMIZATION OF RISER TYPE INDUSTRIAL FLUID CATALYTIC CRACKING UNIT",** in the partial fulfillment of the requirements of the award of the degree of Master of Technology in Chemical Engineering with specialization in Computer Aided Process Plant Design, submitted in the Department of Chemical Engineering, Indian Institute of Technology Roorkee, Roorkee, Uttarakhand (India), is an authentic record of my own work carried out during the period from July 2006 to June 2007 under supervision of **Dr. I. M. Mishra**, Professor, Department of Chemical Engineering, Indian Institute of Technology Roorkee, Roorkee, and **Dr. Shishir Sinha**, Assistant Professor, Department of Chemical Engineering, Indian Institute of Technology Roorkee, Roorkee, Uttarakhand (India).

I have not submitted the matter, embodied in this dissertation for the award of any other degree or diploma.

Date: 26 June 2007

Place: Roorkee

RAGHVENDRA SINGH

CERTIFICATE

This is to certify that the above statement made by the candidate is correct to the best of my knowledge and belief.

(Dr. I. M. Mishra)
Professor
Department of Chemical Engineering
IIT Roorkee, Roorkee (UA)-247667

(Dr. Shishir Sinha)
Assistant Professor
Department of Chemical Engineering
IIT Roorkee, Roorkee (UA)-247667

CONTENTS

LIST OF FIGURES

LIST OF TABLES

ACKNOWLEDGEMENT

"COMMIT YOURSELF TO CONSTANT IMPROVEMENT AND QUALITY" to what I have tried to do so in this dissertation. To make a good quality report a lot of help was required from professors, seniors, friends, family members, and many more. It's really very difficult to express in few words.

I express my deep sense of gratitude to my guide Dr. I. M. Mishra, Professor, Department of Chemical Engineering, Indian Institute of Technology Roorkee, Roorkee, for his keen interest, constant guidance and encouragement throughout the course of this work, his experience, assiduity and deep insight of the subject held this work always on a smooth and steady course.

I am also extremely thankful to Dr. Shishir Sinha, Assistant Professor, Department of Chemical Engineering, Indian Institute of Technology Roorkee, Roorkee, for his concern and showing keen interest during this course of work.

I thank all well wishers who in any manner directly or indirectly have put a helping hand in any part of this piece of work. .

Above all, I want to express my heartiest gratitude to all my family members for their love, faith and support for me, which has always been a constant source of inspiration.

RAGHVENDRA SINGH

ABSTRACT

Fluid catalytic cracking (FCC) unit plays most important role in the economy of a modern refinery that it is use for value addition to the refinery products. Because of the importance of FCC unit in refining, considerable effort has been done on the modeling of this unit for better understanding and improved productivity. in last sixty years, the mathematical modeling of FCC unit have matured in many ways but the real process whose hardware is ever-changing to meet the needs of petroleum refining. The process is characterized by complex interactions among feed quality, catalyst properties, unit hardware parameters and process conditions.

The FCC unit comprises of three stages: a riser reactor, a catalyst stripper, and a regenerator (along with other accessories). From modeling point of view, the riser reactor is of prime importance amongst these stages. Detailed modeling of the riser is a challenging task for due to complex hydrodynamics and the fact that there are thousands of unknown hydrocarbons in the FCC feed but because of the involvement of different types of reactions taking place simultaneously.

The traditional and global approach of cracking kinetics is lumping. Mathematical models dealing with riser kinetics can be categorized into two main types. In one category, the lumps are made on the basis of boiling range of feedstocks and corresponding products in the reaction system. This kind of model has an increasing trend in number of lumps of the cracked gas components. The other category is that in which the lumps are made on the basis of molecular structure characteristics of hydrocarbon group composition in reaction system. This category of models emphasizes on more detailed description of the feedstock. These models do not include chemical data such as type of reaction and reaction stoichiometry. In the present work, five lump kinetic schemes is considered, where gas oil cracks to give lighter fractions (like gasoline, LPG, dry gas) and coke.

The integrated reactor-regenerator steady state model makes gross assumption about the hydrodynamics, this model equation solved by Runga Kutta method in MATLAB. Rate equations of all the five lumps are integrated along the riser length with a small step size using Runga Kutta method. There are nine kinetic parameters and one catalyst deactivation activity.

The Genetic Algorithm (GA) is a stochastic global search method that mimics the metaphor of natural biological evolution. GAs operates on a population of potential solution applying the principle of survival of the fittest to produce better and better approximations to a solution. At each generation, a new set of approximations are created by the process of selecting individuals according to their level of fitness in the problem domain and breeding them together using operators borrowed from natural genetics. The multi-objective optimization of industrial operations using genetic algorithm and its variants often requires inordinately large amounts of computational (CPU) time. In the present work, the multi objective the binary coded elitist non-dominated sorting genetics algorithm (NSGA-II) is adapted, and the new code, NSGA-II JG is used to obtain solution for the multi-objective optimization of an industrial fluidized bed catalytic cracking unit. This unit is associated with a complex model that is highly compute-intense. The CPU time required, for this problem is found to reduce fivefold, when NSGA-II JG is used, as compared to when NSGA-II is used. This adaptation can prove to be of considerable value for solving other compute intense problems in chemical engineering.

Chapter-1

INTRODUCTION

INTRODUCTION

Fluid Catalytic Cracking is called FCC, and is one of the most representative refining technologies. FCC is generally used as a generic term for an FCC process and FCC unit. The first FCC unit was developed and put into practical use in the United States in the early 1940s, since then many improvements in catalysts and process technologies have been made.

In many refineries FCC is the primary conversion unit. Crude oil as produced from the ground contains hydrocarbons ranging from light gases and LPG to residues boiling above 343°C (650°F). Products of various boiling ranges can be produced by distillation. It converts high molecular weight petroleum fractions (heavy gas oil- portion of crude oil that boils in the range 330-550°C) to lower molecular weight products such as gasoline etc. There are approximately 400 catalytic crackers operating worldwide with a total processing capacity is over 12 millions barrels per day. About 45% of the worldwide gasoline production comes from the FCC and its ancillary units. In spite of its commercial importance optimization of the FCC unit is still largely empirical due to complex interactions between a large number of dependent and independent parameters. Determining optimal operating parameters for different modes of operation by changing process conditions on a commercial FCC is neither feasible nor advisable.

Petroleum refining is a very wide industry. Crude oil is separated into various fuels, lubricants and petrochemical products that these are improve the quality of our life. The refining industry needs to effectively evaluate process performance to identify option of producing desirable products and meeting environmental legislation. The major transformation of mainly producing fuels for transportation to the one which makes different products, such as fuels, chemicals products, specialty products, electricity, hydrogen and so on, which is so called co-production. Basically, a refining plant will be a combination of a chemical plant, fuel producer and a commercial power station.

The crude oil is first separated into several boiling fractions by atmospheric and vacuum distillation units, and then each boiling fraction is further processed by several kinds of catalytic reaction operation such as hydrotreating, hydrocracking, catalytic reforming and catalytic cracking; by non-catalytic reaction operations such as thermal

cracking; and by treatment operations such as the removal of impurities and fine fractionation.

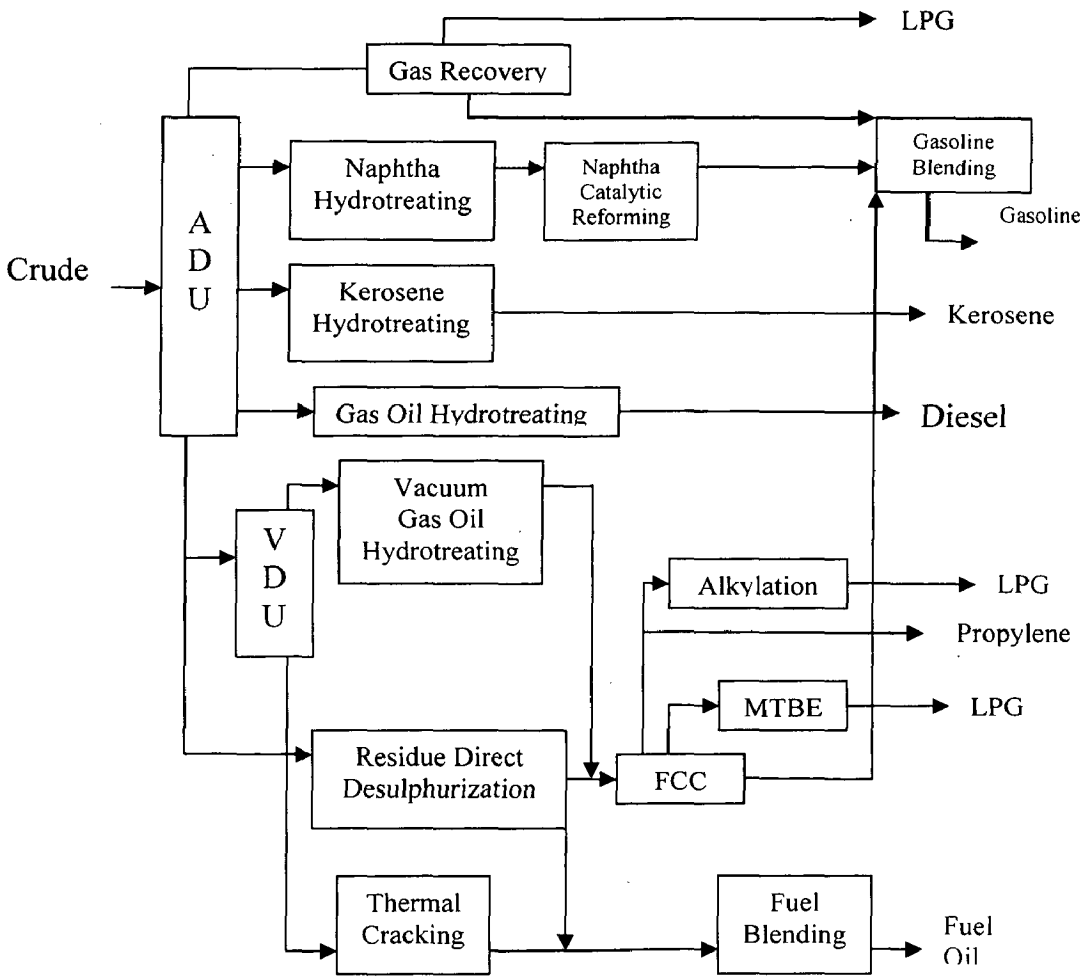

Figure 1.1: Role of FCC in the refining industry

Figure 1.1 shows as the crude oil is distilled in atmosphere distillation unit to produce LPG, naphthas, kerosene and diesel oil. The residue from the atmosphere distillation unit is fed to the vacuum distillation unit where it is separated into vacuum gas oils and vacuum residue. The heavy vacuum gas oil, which normally constitutes 25-30% of the total crude oil volume, is fed to the FCC unit where it is converted into lighter products. The heavy vacuum gas oil (VGO) has a boiling range of 343°C (650°F) to 565 °C (1050°F). In addition to the VGO a wide range of feedstock can be processed in FCC units such as hydrotreated gas oils, cracker gas oils, and deasphalted oils.

1.1 Fluid Catalytic Cracking (FCC) Process

All modern FCC units consists of two basic components, a reactor in which the catalyst is brought in contact with the feed (Gas oil), and a regenerator in which the coke deposited on the catalyst during the cracking reactions is burned off for regenerating the catalyst. A schematic of FCC unit is shown in Figure1.2. Other auxiliary units such as feed preheat and flue gas systems are also required for control and optimal operation of this unit.

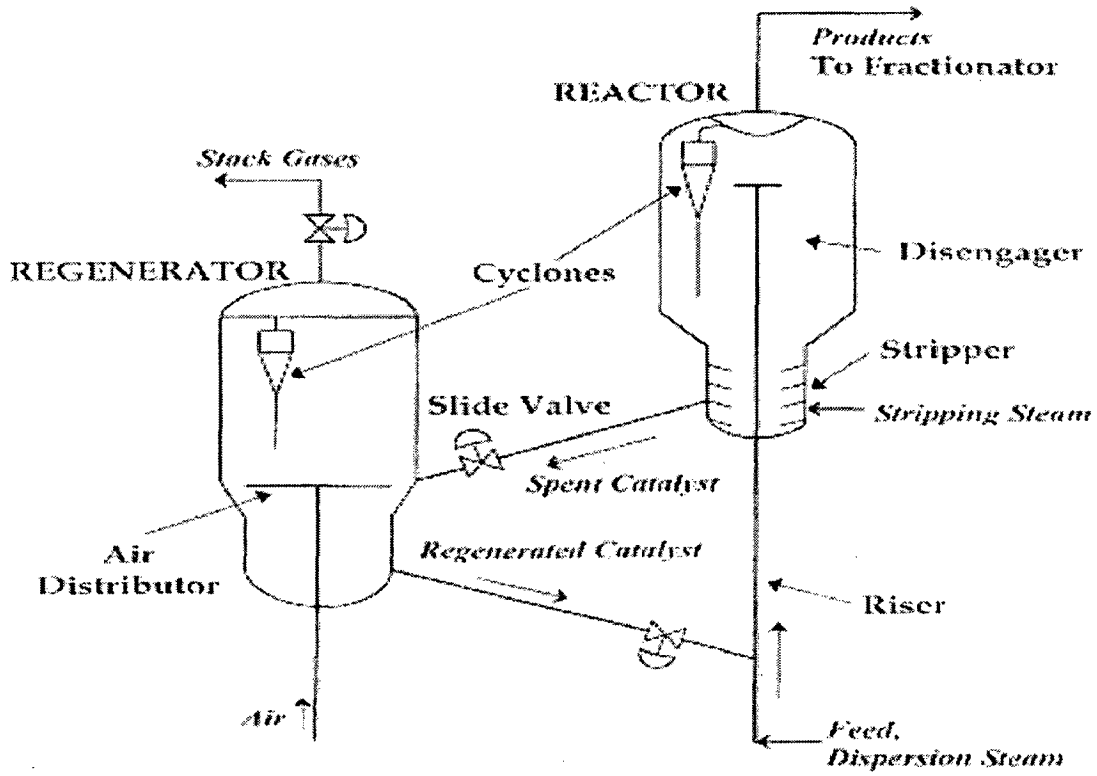

Figure 1.2: Schematic diagram of FCC unit (Han et al., 2001)

1.1.1 Feed Preheat System

The refinery produced gas oil and supplemental feedstocks are generally combined and sent to a surge drum which provides a steady flow of feed to the FCC unit's charge pumps. This drum can also serve as a device to separate any water or vapor that may be present in the feedstocks.

From the surge drum, the feed is normally heated to a temperature of 270-375°C (550-700°F). This is usually done by heat exchanger with intermediate heat removal

pump around from the main fractionators (**Kumar et al. 2005**). While feed preheat system may differ greatly from unit to unit, the feed is normally heated by exchange with the light cycle oil, heavy cycle oil, or bottom pump around. This raises the feed temperature to 150-260°C (300-500°F) which is generally sufficient for the most FCC units. In some cases fired heaters also used to preheat the feed.

1.1.2 Reactor

Almost all reactors presently in use consists of a riser, in which there is short contact time (less than 5 seconds) of catalyst and feed. Virtually all the cracking reactions occur in the riser over this short time period before the catalyst and the products are separated in the reactor. However, some thermal and non-selective catalytic cracking reactions continue to occur in the reactor housing.

From the preheated, the feed enters the riser near the base where it comes in contact with the hot regenerated catalyst coming from the regenerator. The ratio of catalyst to oil is normally kept in the range of 4:1 and 9:1 by weight. The heat carried by the catalyst coming from the regenerator provides the energy to heat and vaporize the feed, and the energy required for the endothermic cracking reactions occurring in the riser (**Ali and Rohani, 1997**). The cracking reactions start instantaneously in the vapor phase as soon as the feed is vaporized. The expanding volume of the vapors that are generated by vaporization and cracking lift the catalyst and carry it up in the riser. Overall these cracking reactions are endothermic and thus, the temperature in the riser decreases as the reaction progresses.

Typical riser dimensions are about half a meter to two meters in diameter and 20-35 meters in length. The ideal riser simulates a plug flow reactor, where the catalyst and the vapor travel along the length of the riser at the same velocity with minimum back mixing. However, in real cases there is considerable slip and back mixing of catalyst particles.

Efficient contact of feed and catalyst is critical for the desired cracking reactions. Steam is introduced to atomize the feed (**Gupta and Subba Rao, 2003**). The atomization of feed increases the availability of feed at the reactive acid sites of the catalyst. In the presence of a high activity zeolite catalyst, virtually all of the cracking reactions take

place in the riser in two or four seconds time frame. Risers are normally designed for an outlet vapor velocity of 15 to 25 m/s, with an average hydrocarbon residence time of about two second (based on outlet conditions). As a consequence of the cracking reactions, a hydrogen deficient material called coke is deposited on the catalyst that reduces its activity.

At the end of the riser, the product vapors and the catalyst flow through a riser termination device (RTD) which separates the catalyst from the hydrocarbon vapors. Quick separation is essential to avoid the undesirable side reactions. The separated catalyst is then directed to the spent (deactivated) catalyst stripper. Hydrocarbon vapors from the RTD enter the reactor vessel. In modern cracking units, the reactor vessel plays only a minor role in actual cracking reactions. In fact, the reactions occurring in this vessel are generally considered to be undesirable. The primary function of this reactor vessel now a day is to be providing some disengagement space between the RTD and the cyclones.

The product vapors entering the reactor from the RTD get mixed steam and stripped hydrocarbon vapors and flow through the reactor cyclones. The reactor cyclones remove the catalyst particles not separated in the RTD. Vapors from the reactor cyclones flow into the main fractionators. Spent catalyst from the RTD and the reactor cyclones flows into the spent catalyst stripper. Here the catalyst is contacted with steam to strip off the vapors adsorbed on the catalyst. Baffles are provided in the stripper to improve the mixing between steam and catalyst.

1.1.3 Regenerator

The spent catalyst from the stripper flows to be regenerator through a slide valve. This valve serves to control the level of catalyst bed in the stripper. The regenerator has two main functions: it restores the catalyst activity and supplies heat to crank the feed. The spent catalyst entering the regenerator contains between 0.8 and 0.25 wt% coke, depending on the quality of the feedstock. Components of coke are carbon, hydrogen and the trace amounts of sulphur and nitrogen.

Air is the source of oxygen for the combustion of coke and is supplied by a large air blower. The air blower provides sufficient air velocity and pressure to maintain the

catalyst bed in fluid state. The air enters the regenerator through an air distributor located near the bottom of the vessel. The catalyst and air are well mixed in a fluid bed (or fast fluid bed) and the carbon (coke) deposited on the catalyst during the cracking reactions is burned off (**Krishna et al., 1985**). The heat produced by the combustion of coke raises the temperature of the catalyst which in turn is used for supplying the heat required by the cracking reactions. Flue gases leaving the regenerator pass through the regenerator cyclones where entrained catalyst is removed and return back to the regenerator.

Hot regenerator catalyst from the regenerator enters the riser through a slide valve. This valve controls the quantity of hot catalyst entering the riser and thus the riser outlet temperature

1.1.4 Flue gas system

The hot flue gas leaving the regenerator contains an appreciable amount of energy. A number of heat recovery schemes are used to recover this energy. In some units, the flue gas is sent to a CO boiler where both sensible and the heat of combination are used to generate high pressure steam (**Kumar et al., 2005**). In other units, the flue gas exchange heat with boiler feed to produce steam via the use of shell/ tube or box heat exchangers.

1.1.5 Catalyst handling

Catalyst particle are smaller than 20 microns escape from the reactor and regenerator vessels. The catalyst fines escaping the reactor collect in the fractionator's bottom product storage tank. The recoverable catalyst fines, the existing in the regenerator are removed by the electrostatic precipitator. The catalyst losses are related mainly to hydrocarbon vapor and flue gas velocities, the catalysts, physical properties, and attrition.

The activity of the catalyst degrades with time. The loss of activity is attributed to the impurities in the FCC feed, such as nickel, vanadium, and sulphur, and to thermal and hydro-thermal deactivation. (**de Lasa et al., 1991**). To maintain the desired activity, fresh catalyst is continually added to the unit. Fresh catalyst is stored in a fresh catalyst hopper and in most units, is added automatically to the regenerator via a catalyst loader.

The circulating catalysts in the FCC unit are called equilibrium catalyst, or E-cat. Periodically, quantities of equilibrium catalyst are withdrawn.

1.2 Evolution of the Fluid Catalytic Cracking (FCC) Technologies

Table 1.1 shows that the technologies for cracking processes were improved in the following steps, from the thermal cracking processes without a catalyst (bath-wise to continuous operation) to the fixed bed catalytic cracking process with a catalyst (cyclic catalyst regeneration) and then changed to the moving bed catalytic cracking process (continuous catalyst regeneration) (**Schaefer, 1989**). After that we arrived at the age of FCC development and enhancement.

Table 1.1: Shows the evolution of FCC (Radar and Mari Lyn, 1996)

Year	Evolution of FCC
1915	McAfee of Gulf Co. Discovered that a Friedel-Crafts Aluminum Chloride Catalyst could Catalytically Crack Heavy Oil.
1936	Use Of Natural Clays as Catalyst could Greatly Improved Cracking Efficiency.
1938	Catalyst Research Associates (CRA) was Found. The Original CRA Members were: Standard Of New Jersey (Exxon), Standard Of Indiana (Amoco). Anglo Iranian Oil Company (BP Oil). The Texas Company (Texaco), Royal Dutch Shell, Universal Oil Products (UOP), The M.W. Kellogg Company, And I.G. Farben (Dropped In 1940).
1942	First Commercial FCC Unit (Model-I Upflow Design) Started Up at Standard of New Jersey's Baton Rouge, Louisiana, Refinery.
1943	First Model-II Down-Flow Design FCC Unit was Brought On-Line. First Thermal Catalytic Cracking (TCC) Brought On-Line.
1947	First UOP Stacked FCC Unit was Built. Kellogg Introduced the Model-III FCC Unit.
1948	Davidson Division Of W.R. Grace & Co. Developed Micro-Spheroidal FCC Catalyst.
1950	Evolution of Bed-Cracking Process Designs.
1951	M.W. Kellogg Introduced the Orthoflow Design.

1952	Exxon Introduced The Model-IV.
1954	High Alumina (Al_2O_2) Catalysts were Introduced.
1955	UOP Introduces Side by Side Design.
1956	Shell Invented Riser Cracking.
1961	Kellogg and Philips Developed and Put the First Resid Cracker Onstream at Borger, Texas.
1964	Mobil Oil Developed USY and Rey FCC Catalyst. Last TCC Unit Completed.
1972	Amoco Oil Invented High Temperature Regeneration.
1974	Mobil Oil Introduced CO Promoter.
1975	Phillips Petroleum Developed Antimony for Nickel Passivation.
1981	TOTAL Invented Two-Stage Regeneration for Processing Residue.
1983	Mobil Oil Reported First Commercial Use of ZSM-5 Octane/Olefins Additive in FCC.
1985	Mobil Oil Started Installing Closed System in its FCC Units.
1994	Coastal Corporation Conducted Commercial Test of Ultrashort Residence Time, Selective Cracking.
1996	ABB Lumus Global Acquired Texaco FCC Technologies.

When the first FCC unit was developed around 1945, the fixed bed Houdry process was still boasting of its own superiority for the catalytic cracking process. Further improvement of the Houdry process was realized by developing the moving bed catalytic cracking process (TCC and Houdry Flow process). On the other hand, companies that took up the challenge of developing a new process which would supersede the Houdry process included Standard Oil (New Jersey), M.W. Kellogg, Standard Oil (Indiana), British Petroleum, Royal Dutch/Shell Group, Texaco, and UOP. These companies promoted research on catalytic cracking with the common possession and formed the world's largest scientific and engineering manpower group at the time, employing about 1000 personnel in all.

Major R&D tasks of this group were shortening catalytic contact time in a catalytic reaction, equalizing temperature in the catalyst bed, and moving a large volume of catalyst efficiently. During these development activities, catalyst fluidization

technology attracted their attention. Furthermore for military reasons at the initial stage of World War II, the pace of development of equipment and construction was much speeded up.

In 1940, at the Baton Rouge refinery of Standard Oil (Louisiana), a 100-BPSD pilot plant was constructed and achieved satisfactory result in tests of a fluid solid moving system (**Schaefer, 1989**). The test results were immediately adopted in tests of a fluid solid moving system. The test results were immediately adopted in the design in the actual plant. This was called the Upflow Type (Model I), in which catalysts rise in the reactor and regenerator and exit from the vessel tops.

Later 1944, the diameter of the reactor and regenerator were expanded and separation of catalysts from vapor was carried out inside the vessels. The catalysts were further in the dense phase and the flow was improved so that catalysts were withdrawn downward from the vessel bottoms (**Schaefer, 1989**). This was called the Downflow Type (Model II). In addition the shapes of catalysts were improved and small spherical shapes came into use significantly decreasing catalyst attrition and improved cyclone efficiency.

In Model I, the economic C/O ratio (catalyst/oil) was about 3 at the maximum limit, but in Model II it was possible to design the ratio technically and economically within the range 3-30.

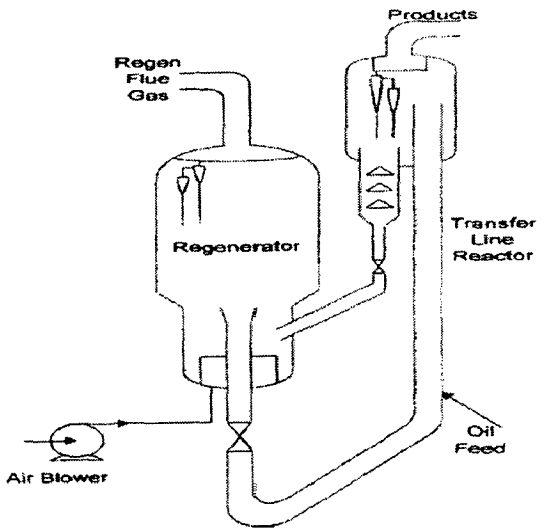

Figure 1.3: Typical schematic Exxon's flexicracker (Radar and Mari Lyn, 1996)

Later in 1946, Model III of the pressure balance type was developed by M.W. Kellogg. On the other hand, the first stacked type FCC unit of UOP design started operation in 1947. Later in 1951, the first M.W. Kellogg Ortho-flow type of FCC commenced operation.

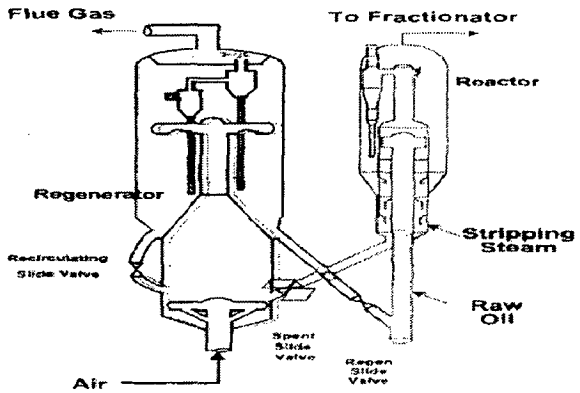

Figure 1.4: UOP FCC unit (Radar and Mari Lyn, 1996)

Standard Oil (New Jersey) also created a new type of unit called Model IV by modifying Model II with the first Model IV unit going into operation in 1952. A number of units of this type are still in operation, including the Esso refinery in Port-Jerome (France).

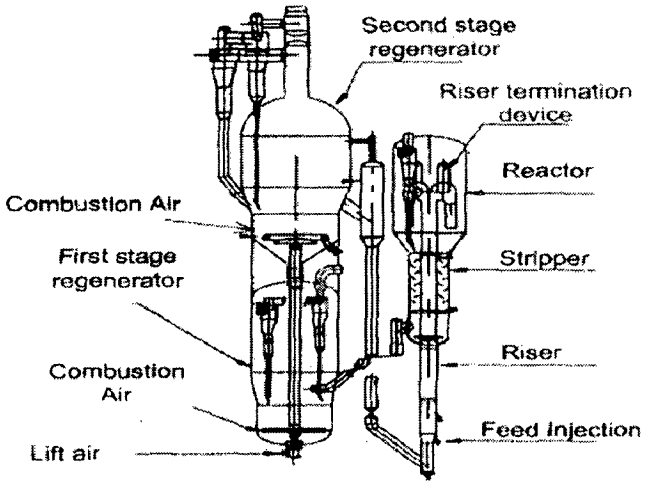

Figure 1.5: SWEC stacked FCC unit (Radar and Mari Lyn, 1996)

1.3 Fluid Catalytic Cracking (FCC) Catalyst

The FCC catalyst is the heart and soul of the process. Both chemical and physical properties of the catalyst properties of the catalyst determine how the FCC unit is

designed and operated. Since fresh catalyst is added to the FCC unit regularly, and catalyst is also withdrawn and lost through cyclone systems, the most important catalyst properties to FCC operation are those of the equilibrium catalyst (**Ye-Mob Chen, 2003**). The catalyst used in the catalytic cracking process is a fine powder made-up primarily of alumina and silica. The particles of this powder are in the size range of 10-140 microns. In appearance it might be somewhat analogous to commercial talcum powder.

Two types of catalysts are currently significant like amorphous and zeolite. The synthetic amorphous catalyst is formed by the precipitation of silica to form a highly porous structure, alumina is added as a surface coatings. Active sites which are acidic in nature are formed at the silica-alumina interface and reaction takes place at these sites with the available hydrogen (**Takatsuka and Minami, 1998**). Zeolite is formed through the reaction of reactive forms of alumina and silica. The reaction conditions are controlled so that the product of the reaction is to be caged like crystalline structure. Zeolite due to their uniform pore structure, have high cracking activities. The refineries which are programmed for gasoline maximization use zeolite catalysts because of their higher activity (50-100 times as amorphous) and improved stability.

A modern FCC catalyst includes the four major components. They are zeolite, matrix, binder, and filler. The first component, zeolite, is the primary active ingredient of the FCC catalyst, which can vary in the range of 15 to 50 wt% of the catalyst. It is a molecular sieve with a well-defined lattice structure, which provides the selectivity to allow only a certain size range of hydrocarbon molecules to enter the catalyst lattice structure. The acidic sites on the zeolite provide most of the activity of the FCC catalyst. The basic building blocks of zeolite are silica and alumina tetrahedra. The second component matrix also contains alumina but mostly in amorphous form, which is another source of the catalyst activity. The function of matrix is to provide active sites in larger pores in the amorphous form of alumina, which allow larger hydrocarbon molecules to diffuse in and crack into smaller molecules. This pre-cracking function of the matrix enables FCC catalyst to process heavier feedstock with large hydrocarbon molecules, which are otherwise unable to enter the zeolite structure. The last two components, the filler and the binder, provide the physical integrity and mechanical strength of the FCC catalyst.

In order to minimize non selective post riser cracking many refiners are revamping their units to operate in the so-called "Short Contact Time" mode. In the FCC operation, catalyst and feed are contacted at the bottom of the riser with cracking reaction proceeding along length of the riser. At the end of riser, the catalyst and products are separated in the disengager. In short contact time mode the catalyst having the some important characteristics are shorter catalyst/oil contact time, higher reactor temperature, higher catalyst circulation rate, and lower regenerated catalyst temperature (**Diddams et al., 1998**). The zeolite component within the catalyst has the greatest effect on activity and therefore, proper zeolite selection is very important. In addition, it is very important to choose a matrix with the right level of activity for a particular application to address the reduction in bottoms upgrading that occurs with shorter contact time. Excess matrix activity is undesirable because it leads to poorer coke and gas selectivities. In addition to providing bottoms cracking activity, matrix should be selected to provide low coke and gas selectivites, particularly in the presence of contaminant metals.

In the particular application area like the production of light olefins (Propylene and butylene) which have driven the recent growth of ZSM-5 usage in FCC units worldwide. A major structural property of ZSM-5 zeolite is shape selectivity, which limits the access of multi-substituted aromatics. According to different authors (**Buchanan, 2000, den Hollander et al., 2002a, b**) tridimensional pores allows circulation across the porous structure of linear compounds whose molecular weight is higher than gasoline. This increase accessibility explains the high conversion in the cracking of polyolefins dissolved in LCO (**Arandes et al., 2002**). Under the FCC conditions these polyolefins undergo thermal cracking in the matrix meso and macro pores and on the external surface of the catalyst particles. When the concentration of polyolefins in the feed is not excessive, this thermal cracking is adequate for the resulting chains to access the porous structure of the HZSM-5 zeolite, where catalytic cracking takes place in earnest.

1.4 Modeling of Fluid Catalytic Cracking (FCC) unit

Modeling is powerful tool in present day refineries and is used for a variety of applications. Because of the importance of FCC unit in refining, considerable effort has

been done on the modeling of this unit for better understanding and improved productivity. In last fifty years, the mathematical modeling of FCC unit have matured in many ways but the modeling continues to evolve to improve the closeness of models prediction with the real process whose hardware is ever-changing to meet the needs of petroleum refining. Complexity of the FCC process because of unknown reaction mechanism, complex hydrodynamics and strong interaction between reactor and regenerator has made it almost impossible to develop a general model for the integrated process. Therefore, researchers in this field have worked on different aspects of the process separately for modeling purposes (**Kumar et al., 2005**). However, maximum attention has been paid on the modeling of the riser reactor which is the most important part of the FCC unit.

The level of detail of the model depends on the unit being modeled and the end use of the model. Simple linear input output models are used for inventory control, energy audit and for overall refinery optimization. On the other hand, design of a new unit may require very sophisticated models which accounts for hydrodynamics, heat and mass transfer, reaction phase equilibrium, strength of materials, corrosive properties of fluids to be handled, etc. Rating the performance of a unit or optimization of its operating conditions call for steady state models which are analytical and non linear and includes the physics of the process to a reasonable extent.

Gas oil consists of a large number of hydrocarbons normal and iso-paraffins, napthenes, aromatics, substituted (or alkyl) aromatics and condensed ring compounds. The cracking reaction kinetics will depend on the type of the hydrocarbon and the number of carbon atoms present in a molecule but due to lack of information of detailed FCC feed composition; such a detailed kinetic model is not practical. The approach followed is that the feed and products are characterized in terms of a small number of groups of hydrocarbons which are similar in nature and each of these groups of hydrocarbons which are similar in nature and each of these groups could be taken to behave like a single kinetic entity called a kinetic lump.

All these mathematical models are based on lumping scheme in which FCC feed and products are assumed to be made of a few number of the lumps and kinetic parameters are estimated empirically for the conversion of one lump to the other. In the

present work, basically the model formulation in lumping scheme, a five lumping scheme model (**Ancheyta et al., 1999**) presents an improved and updated model for modern fluidized bed catalyst cracker (FCC). The separation of coke as separate lump is important as the coke supplies the heat for the endothermic cracking reactions. The C_1-C_4 gas yield increase with the increasing reaction temperature at the expense of the yield of gasoline and coke. The rate constant and activation energies for the reaction scheme are obtained by regression using the experimental data. **Martin et al., (1992), Ancheyta et al., (1999), Hagelberg et al., (2002)** and **Bollas et al., (2006)** for their studies of various aspects of FCC modeling.

1.5 Optimization Technique

The FCC unit is a complex process because it is a multiunit process with significant nonlinear and non-stationary behavior. The conventional approach to controlling a FCC unit involves control of the reactor temperature and the flue gas oxygen concentration using the catalyst circulation rate and the regenerator air flow rate respectively.

The Genetic Algorithm (GA) is a stochastic global search method that mimics the metaphor of natural biological evolution. GA operates on a population of potential solution applying the principle of survival of the fittest to produce better and better approximations to a solution. At each generation, a new set of approximations is created by the process of selecting individuals according to their level of fitness in the problem domain and breeding them together using operators borrowed from natural genetics (**Dave and Saraf, 2003**). This process leads to the evolution of populations of individuals that are better suited to their environment than the individuals that they were created from, just as in natural adaptation.

Individuals or current approximations are encoded as strings, *chromosomes*, composed over some alphabet(s), so that the *genotypes* (chromosome values) are uniquely mapped onto the decision variable (*phenotypic*) domain. The most commonly used representation in GA is the binary alphabet {0, 1} although other representations can be used, e.g. ternary, integer, real-valued etc. For example, a problem with two

variables, x1 and x2 may be mapped onto the chromosome structure in the following way:

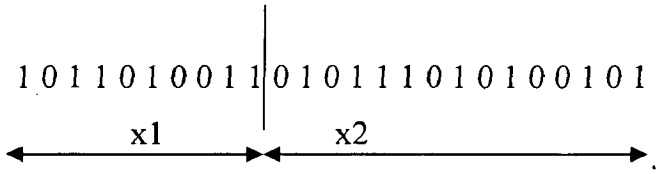

Where, x1 is encoded with 10 bits and x2 with 15 bits, possibly reflecting the level of accuracy or range of the individual decision variables. Examining the chromosome string in isolation yields no information about the problem, we are trying to solve. It is only with the decoding of the chromosome into its phenotypic values that any search process will operate on this encoding of the decision variables, rather than the decision variables themselves, except, of course, where real-valued genes are used.

It is having decoded the chromosomes representation into the decision variable domain, it is possible to asses the performance, or fitness, of individual members of a population (**Kasat et al., 2002**) This is done through an objective function that characterizes an individual's performance in the problem domain. In the natural world, this would be an individual's ability to survive in its present environment. Thus, the objective function establishes the basis for selection of pairs of individuals that will be mated together during reproduction.

During the reproduction phase, each individual is assumed a fitness value derived from its raw performance measure given by the objective function. This value is used in the selection to bias towards more fit individuals. Highly fit individuals, relative to the whole population, have a high probability of being selected for mating whereas less fit individuals have a correspondingly low probability of being selected.

Once the individuals have been assigned a fitness value, they can be chosen from the population, with a probability according to their relative fitness, and recombined to produce the next generation (**Han et al., 2001**). Genetic operators manipulate the characters (genes) of the chromosomes directly using the assumption that certain individual's gene codes, on average produce fitter individuals. The recombination operator is used to exchange genetic information between pairs, or larger groups, of

individuals. The simplest recombination operator is that of single point crossover. Consider the two parent binary strings

$P_1 = 1\ 0\ 0\ 1\ 0\ 1\ 1\ 0$

$P_2 = 1\ 0\ 1\ 1\ 1\ 0\ 0\ 0$

If an integer position, i is selected uniformly at random between 1 and the string length, l minus one [1, l-1] and the genetic information exchanged between the individuals about this point then two new offspring are produced. The two offspring below are produced when the crossover point i=5 is selected.

$Q_1 = 1\ 0\ 0\ 1\ 0\ 0\ 0$

$Q_2 = 1\ 0\ 1\ 1\ 1\ 1\ 0$

This crossover operation is not necessarily performed on all strings in the population. Instead, it is applied with a probability P_x when the pairs are chosen for breeding. A further genetic operator, called mutation, is then applied to the new chromosomes, again with a set probability; P_m. Mutation causes the individuals genetic representation to be changed according to some probabilistic rule. In the binary string representation, mutation will cause a single bit to change its state, $0 \rightarrow 1$ or $1 \rightarrow 0$. So, for example, mutating the fourth bit of O_1 leads to new string,

$O_{1m} = 1\ 0\ 0\ 0\ 0\ 0\ 0\ 0$

Mutation is generally considered to be a background operator that ensures the probability of searching a particular subspace of the problem space is never zero. This has effect of tending to inhibit the possibility of conveying to a local optimum, rather than the global optimum.

After recombination and mutation, the individuals strings are then, if necessary, decoded the objective function evaluated a fitness value assigned to each individuals and individuals selected for mating according to their fitness and so the process continues through subsequent generations (**Dave and Saraf, 2003**). In this way, the average performance of the individuals in a population is expected to increase as good individuals are preserved and bred with one another and the less fit individuals die out. The GA is terminated when some in the population, or when a particular point in the search space is encountered.

Chapter-2

Literature Review

LITERATURE REVIEW

Because of the importance of FCCU in refining, considerable effort has been put into the modeling of this unit. In last five decades, the mathematical modeling of FCC units has matured in many ways but the modeling continues to evolve to improve the closeness of models predictions to the real process whose hardware is ever-changing to meet the needs of petroleum refining. The complexity of the FCC process because of unknown reaction mechanism, complex hydrodynamics and strong interaction between reactor and regenerator, has made it almost impossible to develop a general model for the integrated process.

Process models are must for the design, optimization and control of commercial plants. In addition they provide guidance in the development of a new process and can reduce both time and capital requirements. The utility of a process model depends strongly on its predictive capabilities. The predictions should be reliable over wide ranges of charge stock compositions and process conditions. The result will provide an understanding of the chemical reactions involved and lead to the development of improved catalysts and processes. Therefore researchers in this field have worked on different aspects of the process separately for modeling purposes.

2.1 Modeling of Riser Reactor

Modeling of the riser reactor of an FCC unit is quite complex because of the presence of all three phases (solid, liquid and vapor) in the riser, involvement of physical and chemical rate steps, and its strong interaction with the regenerator. **Wei and Kuo (1969)** had shown that it was possible to lump a number of species together and still have the lumped kinetics accurately describe the overall reaction behavior of the system. They referred to this as exact lumping and went on to show that other systems might be partially lumpable with only small, expectable errors being introduced.

Several workers make considerable efforts in all the above aspects of riser modeling. **Gupta and Subba Rao (2001)** have given summary of main features of some FCC riser models. (Table 2.1)

Table 2.1: Summary of main features of some FCC riser models (Gupta and Subba Rao, 2001)

Type	Corella and Frances (1991)	Martin, Derouin, Forissier, Wild, and Bernard (1992)	Flinger, Schipper, Sapre and Krambeck (1994)	Ali, Rohani and Corriou (1997)	Derouin, Navicato, Forrissier, Wild, and Bernard (1997)	Theologos, Lygeros, and Markatos (1999)
Vaporization	Instantaneous	Instantaneous	Instantaneous	Instantaneous	Instantaneous	Vaporization followed by cracking
Temperature variation	Adiabatic	Isothermal	Isothermal	Adiabatic	Isothermal	Adiabatic
Molar expansion	Considered	Considered	Not considered	Not considered	Considered	Not considered
Axial catalyst holdup	Slip factor varied between values 1.15 and 1.05 along riser height	Correlation relating slip factor to riser height fitted to plant data	Cluster model approach	Constant	Correlation relating slip factor to riser height fitted to plant data	Single particle dynamics
Mass transfer resistance	Not considered	Not considered	Fitted to plant data	Not considered	Not considered	Not considered
Kinetic model	Five lump	Five lump	Three lump	Four lump	Nineteen lump	Three lump
Deactivation	Non-selective, based on the time-on – stream of catalyst	Non-selective, based on the coke concentration on catalyst	Non-selective, based on the time-on-stream of catalyst	Variation along riser height not considered	Non-selective except reactions leading to coke formation, based on coke concentration on catalyst	Non-selective, based on the time-on-stream of catalyst

2.1.1 Riser Kinetics

Describing the kinetics mechanism for the cracking of petroleum fraction has been still is a challenge for the researchers in the field of modeling of the fluid catalytic cracking. The presence of thousands of unknown components in the feed to the riser and the parallel/ series reactions of these components makes the kinetics modeling difficult. The following classification of important chemical reactions occurring during catalytic cracking was listed by **Gates et al., (1979)**:

a) Alkanes Cracking

$$C_nH_{2n+2} \longrightarrow C_mH_{2m} + C_pH_{2p+2} \quad \text{with } n = m+p \qquad (2.1)$$

b) Alkenes Cracking

$$C_nH_{2n} \longrightarrow C_mH_{2m} + C_pH_{2p} \quad \text{with } n = m+p \qquad (2.2)$$

c) β- scission of aromatic alkyl chains

$$ArC_nH_{2n+1} \longrightarrow ArC_mH_{2m-1} + C_pH_{2p+2} \quad \text{with } n = m+p, \qquad (2.3)$$

And Ar is aromatic ring

d) Cycloalkanes Cracking

$$\text{Cycloalkane + alkanes} \longrightarrow \text{aromatic + alkanes} \qquad (2.4a)$$

$$\text{Coke Precursor + alkanes} \longrightarrow \text{coke + alkanes} \qquad (2.4b)$$

e) Isomerization

$$\text{Alkenes} \longrightarrow \text{branched alkene} \qquad (2.5)$$

f) Condensation reactions

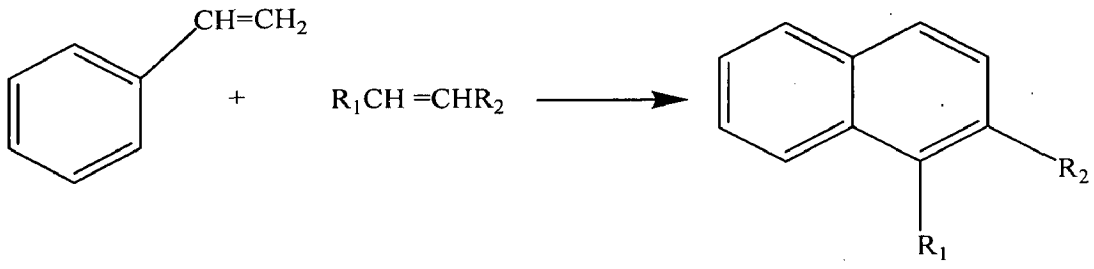

(2.6)

Weekman and Nace (1970) developed a simple kinetic scheme based on the theory of Wei and Prater (1963) for the kinetic modeling of cracking reactions occurring in the riser reactor. This work can be considered as pioneer in developing the simple kinetic mechanism for FCC modeling purposes. Authors divided the charge stock and products into three components, namely the original feedstock the gasoline (boiling range C_5 410°F) and the remaining C_4's (dry gas and coke) and hence simplified the reaction scheme the model predicted the conversion of gas oil (feed stock) and gasoline yield in isothermal condition in fixed , moving, and fluid bed reactors.

The kinetic parameters of the model were evaluated using the experimental data. Since the gas oil and gasoline cracking rates have different activation energies an optimum reactor temperature was also determined for the system. The different authors were descried the different kinetic scheme as follows below:

a. **Blanding (1953)** treated the kinetics of catalytic cracking using a one lump conversion model. A study of factors affecting the extent of the reaction is summarized based on the experimental data obtained in developing the fluidized catalytic process. Equations for characterizing the reaction show the rate at constant pressure to be about proportional to the second power of the fraction of the unconverted feed.
b. **Weekman et al. (1968)** proposed the two lump kinetic schemes, in which the feed and the product were considered. Later, since the prediction of gasoline was an important as that of conversion, **Weekman et al. (1969)** proposed another model, in which the products were divided into two lumps: one corresponding to gasoline and the other to coke and dry gas.
c. The three lump models of **Weekman and Nace (1970)** were capable of predicting gasoline yield. However it ignored the important aspect of prediction of coke deposition on the catalyst surface. The main limitation of this model is that it can not predict coke yield separately and hence this model does not allow heat integration with regenerator unit.
d. **Lee et al. (1989a)** proposed a four lump kinetic model by separating the coke from the three lumps of **Weekman and Nace (1970)** as a separate lump. The separation of coke as a separate lump was important as the coke supplies the heat

for the endothermic cracking reactions. Authors also concluded that the schemes were obtained by regression using the experimental data of **Wang (1974).** This four lump model because of its simplicity and ease of formulation and solution of kinetic, material and energy equations, was used by **Farag et al (1993), Zheng (1994), Ali and Rohani (1997), Blasetti and de Lasa (1997), and Gupta and Subba Rao (2001)** for their studies of various aspects of FCC modeling.

e. **Ancheyta et al. (1999)** proposed a five lump kinetic scheme, in which gas lump was further split into dry gas and LPG. The model includes the seven rate constant, **Martin et al. (1992)** reported another five lump kinetic scheme for vacuum gas oil cracking, in which feed was considered as heavy cycle oil and the product lumps were light cycle oil, gasoline, gases and coke.

f. The kinetic constancy for various possible reactions of the ten lump models of (**Gross et al., 1976**).The rate constants of the model were determined using the experimental data obtained in a fluidized dense bed with a commercial FCC catalyst.

g. **Jacob et al. (1976)** followed the approach of kinetic lump schemes who used ten lumps describe the feed and the cracking products. The ten lumps model requires a detailed feed characterization in terms of eight lumps which call for use of sophisticated analysis tools like mass spectroscopy, gas chromatography, silica gel precipitation etc., which is not practical on a routine basis. This detailed kinetic model was further extended by **Oliveira (1987)** proposed a twelve lump scheme in which the coke lump of ten lump scheme of **Jacob et al. (1976)** is divided into two gas lump (gas1 and gas 2) and a coke lump.

h. A thirteen lump reaction scheme was proposed by **Sa et al. (1995),** considering coke and cracking gas as two separate lumps and dividing the aromatic part of the vacuum residue into two parts, one of which is in resin and aspartames fraction, other in saturate and aromatic fraction. This kinetic scheme was used by **Gao et al. (1999)** for their turbulent gas-solid flow and reaction model in FCC riser reactor.

i. **Pitault et al. (1994)** developed a nineteen lump kinetic model, comprising twenty-five chemical reactions. This nineteen lump kinetic model was used by Derouin based on molecular approach comprising twenty-five chemical reactions.

This nineteen lump kinetic model was used **Derouin et al. (1997)** in their hydrodynamic model for the prediction of FCC products yields for an industrial FCC unit. Table: 2.2 show the kinetic constant (of lumped schemes) obtained by various authors.

Another method of kinetic modeling is the single events method given by **Feng et al. (1993).** It permits a mechanistic description of catalytic cracking. It is based on the detailed knowledge of the mechanism of various reactions involving the carbon ions. Determine of the kinetic constant for these single event requires some reaction of pure hydrocarbon. Based on the above method, **Dewachtere et al. (1999)** developed a kinetic model for catalytic cracking of vacuum gas oil in terms of elementary steps of chemistry. The lumping was done such that a link with modern analytical techniques is possible. For the network generation, in each lump all likely chemical species are considered and accounted for.

Table: 2.2 Values of kinetic constant obtained with commercial FCC catalysts

Authors	T, K	K_0, s^{-1}	K_1, s^{-1}	K_2, s^{-1}
Weekman (1968)	755	6.3×10^{-3}	5×10^{-3}	5×10^{-4}
Nace et al. (1971)	755	2.8×10^{-3} to 1.1×10^{-2}	2.2×10^{-3} to 9.3×10^{-3}	3.3×10^{-4} to 2.8×10^{-3}
Parakos et al. (1976)	783-811	0.36-0.70	0.27-0.52	0.03-0.52
Corella et al. (1985)	793	0.19	0.12	6.6×10^{-3}
Corella et al. (1986)	773	0.23	0.18	3.2×10^{-2}
Lee at al. (1989)	755-888	5.63×10^{-3} to 3.15×10^{-3}	4.34×10^{-3} to 2.2×10^{-2}	2×10^{-4} to 6.86×10^{-4}

K_0 = kinetic constant for the cracking reaction of gas oil

K_1 = kinetic constant for the formation from gasoline from gas oil

K_2 = kinetic constant for the formation of gases from gas oil.

Other efforts in the kinetic modeling include:

(a) A strategy to estimate kinetic constants of a lumped reaction, by using the data obtained at 480°C, 500°C ad 520°C in a micro-activity reactor that decreases the number of parameters to be estimated simultaneously for the three lump, four lump and five lump kinetic models (**Ancheyta et al., 1997**).

(b) A study on the effects of metal traps in a FCC catalyst contaminated with high levels of nickel and vanadium (3000 ppm Ni and 4500 ppm V) using pulse reaction technique for testing of FCC catalyst in a down-flow micro activity reactor a different carrier gas flows (120-150ml/min, at STP) and different temperatures (510-550°C) (**Farag et al., 1993**). The four lump kinetic models were used to describe the gas conversion and the yields of gasoline, light gases, and coke in terms of catalyst activity. The data with FCCT (fluid cracking catalyst with in situ metal traps) showed that the selectively to gasoline as well as the gasoline yield was significantly improved, coke formation was reduced and the gas formation was increased.

(c) A study of sensitivity analysis of Weekman's riser kinetics (**Weekman, 1979**) by **Pareek et al. (2003)** using CATCRACK **(Kumar et al., 1995)**. Authors grouped the rate constants on Weekman's kinetic model in five different categories to demonstrate the advantage of such grouping in fine- tuning the simulator.

More advanced models incorporated kinetics and other physical rate steps using advanced computational techniques. **Gupta and Subba Rao (2001)** described the model for the performance of a FCC riser reactor in which considers the feed atomization. This model was predicted conversion and yield pattern in FCC riser reactor. The authors considered the heat transfer, gas oil vaporization, catalyst entrainment hydrodynamics, mass transfer, catalytic cracking kinetics and deactivation. The effect of the initial average droplet size generated by feed atomization nozzle on conversion and yield pattern is discussed. **Gupta and Subba Rao (2003)** described the effect atomization on FCC performance simulation of entire unit. The entire FCC units were simulated by integrating FCC riser model with an FCC regenerator model. The effect of feed atomization on the performance of the unit is evaluated.

Ancheyta et al. (1999) described the 5-Lump kinetic model for gas oil catalytic cracking. In this 5-lump kinetic model is proposed to describe the gas oil catalytic cracking (FCC) process. The model contains eight kinetic constants, including one for catalyst deactivation, taking into account LPG (combined C3 and C4), dry gas (C2 and lighter) and coke yields separately from other lumps (unconverted gas oil and gasoline). Apparent activation energies were determined from experiments obtained in a microactivity reactor (MAT) at temperatures: 480°C, 500°C and 520°C; for a catalyst-to-

oil ratio of 5 using vacuum gas oil and equilibrium catalyst, both recovered from an industrial FCC unit. The model was also predicted the product yields to show good agreement with experimental data.

Peixoto and de Medeiros (2001) used the concept of continuous description of catalytic cracking of petroleum fractions. They are characterized the petroleum fractions using multi indexed concentration distribution function (CDF) developed by **Aris (1989)**. Author used the twelve lump schemes, combined with instantaneous adsorption hypothesis of **Cerqueira (1996)** and deactivation hypothesis of **Oliveira (1987)** in their model. **Bidabehere and Sedran (2001)** developed a model to analyze the simultaneous effects of diffusion, adsorption, and reaction at high temperature inside the particles of commercial FCC catalysts. Authors also experimentally established the relative importance of diffusion, adsorption and reaction using two equilibrium catalysts and n-hexadecane as a test reactant in a riser simulator reactor. **W. Martignoni et al. (2001)** developed the heterogeneous reaction model for FCC riser units. A mathematical model is considered to describe the importance of hydrocarbon species in FCC risers. Results show that both hydrodynamic and the reaction kinetics are strongly influenced by adsorption phenomena. The proposed heterogeneous reaction model predicts increases in catalyst and vapor residence times and consequently higher gas oil conversions.

Hagelberg et al. (2002) described the kinetics of catalytic cracking with short contact times. A novel isothermal pulse reactor was used to study the kinetics of gas oil cracking on a FCC equilibrium catalyst with short contact times. The feed was lighter gas oil than typically used in FCC-units. Experiments were carried out by varying the catalyst-to-oil ratio, volume of the oil pulse, temperature and residence time. After each hydrocarbon pulse the catalyst was regenerated by introducing several oxygen/nitrogen pulses through the catalyst bed. The amounts of carbon monoxide and carbon dioxide formed were measured and the amount of coke on the catalyst was calculated. The reproducibility of the experiments was excellent.

Bowman et al. (2002) described the numerical study of multicomponent vaporization effects in FCC riser reactors. A new vaporization model is incorporated into an existing three phase reacting flow computational fluid dynamics (CFD) code developed at Argonne National Laboratory. In this study ICRKFLO is used to simulate a

low profile FCC riser. A low profile riser has a shorter residence time than standard FCC risers, and the modeling of the droplet vaporization process.

Dupain et al. (2003) discussed the aromatic gas oil cracking under realistic FCC conditions in a microriser reactor. A paraffinic hydrowax feed spiked with naphthalene, anthracene, and phenanthrene was cracked in a once-through microriser reactor at 575°C and with a catalyst-to-oil (CTO) ratio of 4.8 gcat $goil^{-1}$. The conversion by cracking reactions is limited to the paraffinic fraction of the feed and the alkyl groups associated with the benzene ring in aromatic compounds; the aromatic probes did not crack under the applied conditions, and in fact an additional amount of naphthalene was formed by complex dealkylation and hydrogen transfer reactions. The 'uncrackabilty' of aromatics was directly demonstrated by processing aromatic gas oil, containing 33.3 wt% aromatics. Experiments were performed with residence times between 0.05 and 8.2 s, keeping the temperature (525 °C) and CTO ratio (5.5 gcat $goil^{-1}$) constant. The data was interpreted with a simplified first-order five-lump kinetic model, where approximately 19 wt% of the feed was found to be uncrackable.

Chang et al. (2003) described the simulation of FCC riser with multiphase heat transfer and cracking reaction. A validated CFD code ICRKFLO was developed for simulation of three dimensional three phase reacting flows in fluid catalytic cracking (FCC) riser reactors. the numerical technique include a time integral approach to overcome numerical stiffness problems in chemical kinetics rate calculations and a hybrid hydrodynamics kinetic treatment to facilitate detailed kinetics calculations of cracking reaction. ICRKFLO has been validated with extensive test data from two pilot and one commercial FCC units. it is proven to be useful for advance development of FCC riser reactor.

Souza et al. (2003) described the numerical simulation of FCC risers. in this model, to predict the, temperature and concentrations in a FCC riser reactor. A bi-dimensional fluid flow field combined with a 6 lumps kinetic model and two energy equations (catalyst and gas oil) are used to simulate the gas oil cracking process. Based on the velocity, temperature and concentration fields, it is intended, on a next step, to use the second law of thermodynamic to perform a thermodynamic optimization of the system.

Pareek et al. (2003) developed a non isothermal model for the riser reactor which was in corporate in CATCRACK for obtaining the temperature and conversion profiles within the riser reactor. Authors predicted a temperature drop of about 30-40 °C in the riser.

Berry et al. (2004) described the two dimensional reaction engineering model of the riser section of a fluid cracking unit. A two dimensional model that predicts conversion and yield pattern in the riser section of a fluid catalytic cracking unit has been developed. The riser hydrodynamics have been described by the two dimensional model of **Malcus and Pugsley (2002)**. The hydrodynamic model has been modified to make it predictive by incorporating the slip factor for calculation of the cross-sectionally averaged voidage. The model has been coupled with the four-lump kinetic model of **Gianetto et al. (1994)**. To predict how riser operating conditions affect profiles of conversion, yield, temperature, and pressure in the riser.

Kumar et al. (2005) described the new approach of kinetic scheme for the FCC riser is introduced which considers cracking of one lump (Pseudocomponent) giving two other lumps in one single reaction step. the proposed model describe the lumps are formed on the basis of boiling point, but in this approach, each individual lump is considered as a pure component with known physico-chemical properties. Also the reaction stoichiometric is considered. The proposed model also incorporates two phase flow and catalyst deactivation. Since a new cracking reaction mechanism is introduced, a new semi empirical approach based on normal probability distribution is also proposed to estimate the cracking reactions rate constants.

Monroy et al. (2006) described the modeling and simulation of an industrial FCC riser reactor using a lump kinetic model for a distinct feedstock. A process model for an industrial FCC reactor is an important tool for predicting the flexibility to operate with different feedstock within the expected range of conversion, yield of gasoline, and coke production. this steady state model has been developed to describe a two phase transported bed riser reactor that incorporates the stripping section and uses a lump kinetic scheme to account for the cracking of different feedstocks characterized by a paraffin, aromatic, and naphthene content. **Y. Huang et al. (2006)** described the dynamic model of the riser in circulating fluidized bed. The author focuses on modeling the

transient behavior of large CFB units, whose flow characteristics were shown to yield C-shaped voidage profiles using cork as the fluidizing material and air at ambient conditions.

Ramachandran et al. (2007) described the data analysis, modeling and control Performa cement of an industrial FCC unit. Considerable fluctuations were observed in the riser temperature. The undesired occurrence has an adverse effect on the performance of the process unit. The authors developed the tool for analyzing routine operating data in order to characterize the dynamics of the riser temperature and other critical variables that may be affecting the riser temperature.

2.1.2 Riser Hydrodynamics

The riser reactor of FCC unit can be divided into two zones with different functions.

a) The feed-injection zone at the bottom of the riser, where the catalyst particle are accelerated, the evaporation of feed oil takes place and the cracking reactions are initiated.
b) Other zone comprises of the middle and upper sections of the riser (**Gates et al. 1979, Mauleon and Courelle, 1985**).

In the feed injection zone the hydrocarbons fed sprayed in the form of droplet through the feed nozzles comes in contact with the hot regenerated catalyst. The intimate contact between feed and hot catalyst rapidly vaporizes the feed and the increased amount of vapor riser the velocity and lowers the density of the flowing system (**Murphy, 1992**). This part of the riser reactor thus consists of three phases i.e. catalyst (solid), hydrocarbon vapors (gas), and hydrocarbon droplet (liquid). The influx of feed oil, atomizing steam and hot regenerated catalyst result in high velocity, temperature and concentration gradient in this zone

In the middle and upper section, hydrocarbon vapors and solid catalyst are present since all the feed droplet vaporizes after traveling 2-4 m up from the feed inlet (**Gao et al., 2001**). This part of the riser reactor has solid phase (catalyst and coke) and vapor phase (steam, hydrocarbon feed and product vapor). Vapor stream carries with it the catalyst particle in suspension and there is some back mixing of these particles because of slip

between the solid and vapor phase which makes the prediction of solid velocity profile difficult. The slip velocities higher than the terminal settling velocity of a single particle are observed in the riser. This may be attributed to the particle moving in clusters, which are agglomerates of loosely held particles.

Mirgain et al. (2000) studied the feed vaporization models to understand the main physical phenomena in a conceptual mixing chamber, for suggestion the improvement in current FCC technology. Authors demonstrated that feedstock droplet undergo homogeneous vaporization in the gas phase and heterogeneous vaporization as they collide with the catalyst particles. Homogeneous vaporization can not complete vaporize the oil droplets of size greater than 10 μm. On the other hand, if the droplets are sprayed on a dilute suspension or on a dense jet of catalyst particles, the droplet catalyst contact is not proper for heat transfer and vaporization. Thus the best way to ensure fast vaporization of feed droplets in FCC risers and downers is to spray the droplet onto a jet of catalyst particles with voidage ranging 70 to 90 %.

At the riser wall the velocity of the solid and vapor stream is nearly zero and the effect of back mixing is also prominent. The velocity is maximum at the center of the riser. Since the flow in the riser is turbulent, the wall effect is confined to a small portion of the riser cross section. In the rest of the cross section the velocity is almost same. Hence the flow can be divided into two regions; one is a turbulent core region in the center and an annulus region near the wall. A core annulus type of flow pattern in circulating fluidized bed has been shown to exist in several experimental studies (**Capes and Nakamura, 1973, Bader et al., 1988, Tsuo and Gidaspow, 1990, Zhou et al., 1994 and 1995, Samuelsberg and Hjertager 1996, Das et al., 2003**). A radial non-homogeneous distribution of solid particles has also been reported in several other experimental observations (**Weinstein et al., 1986, Hartage et al., 1986**).

Model developed by **Samuelsberg and Hjertager (1996)** predicted core annulus flow riser that was in agreement with the experimental observations of **Miller and Gidaspow (1992)**. Their prediction of maximum velocities in the core and annulus and solid volume fraction profiles agreed with the experimental observations but radial profile of solid and shear viscosity in the core were under predicted. Model predicted the non-homogeneity of velocities, temperature and yield profiles in the riser reactor.

The model of **Werther et al. (1992)** still assumes a core-annulus structure but allows for radial dispersion in the central core, while disregarding gradient in the annular wall zone **Amos et al. (1993)** included radial dispersion in the core zone but the core occupied the entire cross section with the solid particles recycling in a separate region beyond the walls of the vessel.

A cluster/ gas model (**Fligner et al., 1994**) with two phases a cluster phase containing all the particles as spherical cluster. Each of voidage ε_{mf} and a gas phase devoid of particles. Mass transfer is assumed to be controlled by the resistance at the outer surface of the clusters.

Kruse et al. (1995) extended the model of **Shoenfedler et al. (1994)** to include in terms for radial dispersion in both the core and the annulus, with the radial dispersion coefficient assumed to be identical in both zones .These models were further extended by **Sheonfedler et al. (1996a)** to provide for continuous variations throughout the entire cross section.

Ju (1995) developed a Monte Carlo model for a CFB combustor with the riser divided into 40 cells, 20 in the core and 20 in the annulus. Particles are introduced and tracked one by one with particles in the core only able to move upwards or sideways subject to the laws of chance while those in the annulus can only move downwards or sideways. Some particles reaching the top are assumed to be reflected back down the riser. Particles devolatilize and then undergo combustion, allowing the heat release pattern to be approximated by the tracking as few 100 particles.

The probabilistic model of **Abba et al. (2002)** extends the generalized bubbling turbulent model of **Thomson et al. (1999)** to cover the fast fluidization flow regime, allowing for smooth transition from bubbling through turbulent fluidization to fast fluidization. A core- annulus structure is assumed at the fast fluidization terminus with hydrodynamic measurement of regime transition providing estimates of the relative probabilities of each separate flow regime.

In addition there are several CFB reactors models that are unrelated to core-annulus models. These are especially appropriate when the solids concentration and gas velocity are high enough that the dense suspension up flow regime is reached since in the

absence of down flow at the wall there is no reason to be bound by core-annulus representation among these models are the following:

Cell based models (e.g. **Hang et al., 1991, Hyppanen et al., 1993, and Muir et al., 1997**) in which mass and thermal balances allows changes in concentration energy to be tracked as a function of height and time. Several of these models also consider the recirculation loop in which reactants and energy are recirculated and reintroduce near the bottom of the riser.

Bolkan et al. (2003) discussed the hydrodynamic modeling of circulating fluidized bed risers and downers. The simulation results of the both models were verified using the experimental data that had been collected using a state of the art riser and downer pair. The comparison of downer and riser model predictions reveals that downers operate at higher particle velocities and under more dilute conditions than risers and may therefore be better suited for the fast chemical reactions that are rum under dilute conditions. The benefit of downers may be extended if the higher solids holdup observed in risers can be attained through improvements in recycling and feeding particles into the downer.

Werther et al. (2004) developed the modeling of industrial fluidized bed reactors. A modeling approach is presented that is able to handle the most important aspects of industrial fluidized bed reactors. A particular focus is to describe the relationship between catalyst attrition, solids recovery in the reactor system, and chemical performance of the fluidized bed reactor. the completing influences of attrition of the catalyst particles and efficiency of the solids recovery lead to the establishment of a catalyst particle size distribution in the bed inventory, which, in turn influences via the hydrodynamics characteristics of the fluidized bed and thereby, the performance of the chemical reactor.

Huang et al. (2006) discussed the dynamic model of the riser in circulating fluidized bed (CFB). The authors described the transient behavior of large CFB units, whose flow characteristics were shown to yield C-shaped voidage profiles using cork as the fluidizing material and air at ambient conditions. The riser is modeled in two ways: one is the, a set of well mixed tanks connected in series, other is the 1-axisymetric cluster flow. The tanks in series model visualize the riser as consisting of a series of well mixed vessels. When the gas flow rate is constant and solids flow rate changes as a sine wave

function, the voidage along the riser indicates a family of successfully. The cluster flow model assumes that gas and solids flows are unidirectional with no mixing I the axial direction, and the solids move upward in the riser as clusters. This model can be used to predict the smooth changes in voidage profiles for transient process.

2.1.3 Catalyst Deactivation

Catalyst used for the cracking loses in activity mainly due to following three reasons:

1. Physical changes due to coke deposition and structural changes duo to sintering.
2. Poisoning due to the coke presence of metals (nickel and vanadium) and non-metal (sulphur, nitrogen, oxygen) in the FCC feed.
3. Deposition of coke on the active sites.

Catalyst deactivation due to physical changes and metal deposition is irreversible in nature but this deactivation step is very slow. And the fresh catalyst is added periodically to compensate for this loss. Activity loss due to coke deposition is very fast but is reversible and the catalyst can be regenerated easily by burning off the coke deposited on the catalyst surface.

Most of the popular theories on deactivation are based on the time on stream concept. Many researchers have used this concept to formulate various empirical functions to be used for accounting the catalyst decay, since a long time (**Voorhies, 1945, Wojciechowski, 1968 &1974, Nace 1970, Gross et al., 1974**).

Corella and Menendez (1986) developed a model in which the catalyst surface was assumed to be non-homogeneous with acidic sites of varying strength. **Larocca et al. (1990)** reported that catalyst deactivation can be represented by both an exponential decay function and power function with an average exponent of 0.1 to 0.2.

Corella (2004) discussed the modeling of the kinetics of selective deactivation of the catalyst. A selective deactivation kinetic model uses different activity, deactivation function and or deactivation order for teach reaction in the network. Although they reflect reality better than the nonselective models, they may not be useful because of the complexity and handling difficulties.

Bollas et al. (2006) described the Five-lump kinetic model with selective catalyst deactivation for the prediction of the product selectivity in the fluid catalytic cracking process. The catalyst deactivation may affect each one of the reactions in different ways, which creates an additional reason for different variation with time-on-stream of the yield to each product. On the basis of the experimental data of the FCC pilot plant operated in Chemical Process Engineering Research Institute (CPERI, Thessaloniki, Greece), a lumping model was developed for the prediction of the FCC product distribution. The lumped reaction network involved five general lumps (gas oil, gasoline, coke, liquefied product gas, and dry gas) to simulate the cracking reactions and to predict the gas oil conversion and the product distribution. The paths of catalyst deactivation were studied and a selective deactivation model was adopted that enhances the fundamentality and accuracy of the lumping scheme. The hypothesis of selective catalyst deactivation was found to improve the product slates prediction. Models with different assumptions were examined, regarding the behavior of the catalyst, as deactivated, and its effect on the reactions of the lumping scheme. A large database of experiments, performed in the FCC pilot plant of CPERI was used to verify the performance of the models in steady state unit operation. The simulation results depict the importance of incorporating selective catalyst deactivation functions in FCC lumping models.

2.2 Modeling of Regenerator

Regenerator modeling includes three main aspects: hydrodynamics, combustion reaction kinetics and temperature is not a single homogeneous phase, and does not obey a single flow pattern which makes the hydrodynamics challenging, the combustion kinetics poses difficulty because of the unknown composition of the coke deposited on the catalyst surface and also because of the variable CO/CO_2 ratio under different operating conditions.

The phenomenon of multiplicity of steady states (bifurcation behavior) is observed in the FCC units (**Iscol, 1970, Edward and Kim, 1988, Elnashaie and Elshishini, 1990**). The combustion process in the riser are endothermic and kinetics is monotonic it can not be the source of bifurcation behavior. The three steady states known

to exist in the units are high temperature steady state (temperature crucial because of the bifurcation behavior.

2.2.1 Regenerator Kinetics

The reactions taking place in the regenerator are the coke combustion reaction. This coke is the by product of the cracking reactions taking place in the riser and gets deposited on the catalyst surface during the course of cracking. Carbon and hydrogen are the major constituents of the coke that reacts with oxygen, present in hot air entering from the bottom of the regenerator. **Krishna and Perkin (1985)** reported the stoichiometry of the regeneration reaction based on the open literature data and pilot plant studies conducted at Gulf Research and Development Co., Pittsburg as:

$$CH_{x(s)} + [\frac{\beta+2}{2(\beta+1)} + \frac{x}{4}]O_{2(g)} \rightarrow \frac{\beta}{\beta+1}CO_{(g)} + \frac{1}{\beta+1}Co_{2(g)} + \frac{x}{2}H_2O_{(g)} \quad (2.7)$$

And

$$2CO_{(g)} + O_{2(g)} \rightarrow 2CO_{2(g)} \quad (2.8)$$

Where $CH_{x\,(g)}$ is hydrocarbon deposit on the catalyst, β is intrinsic CO/CO_2 ratio at the catalyst site and is given by the following equation

$$\beta = k_{B0}e^{(-E_B/RT)} \quad (2.9)$$

The value of x reported by **Lee et al. (1989b)** to be a number between 0.4 and 2.0. The exact value can be determined from the flue gas analysis. Authors determined this value from the flue gas data collected from Kaohsiung Oil Refinery which came out to be 1.64.

The rate of the carbon combustion is the order with respect to the carbon on catalyst and oxygen partial pressure (**Krishna and Perkin, 1985, Lee et al., 1989b**). The oxidation of CO takes place by two ways with different first order rate constants, one is homogeneous oxidation in the gas phase and the other is catalytic oxidation (**Krishna and Perkin, 1985, Lee et al., 1989b, Arbel et al., 1995**). The rate of CO oxidation is expressed as being first order with respect to the partial pressure of CO and half order with respect to the partial pressure of O_2 for both homogeneous and catalytic oxidation reactions (**Krishna and Perkin, 1985**). The overall rate expression for the CO oxidation

can be obtained by adding the rates of homogeneous and heterogeneous oxidation reactions.

2.2.2 Regenerator hydrodynamics

The spent catalyst from the separator enters into the regenerator unit where it is fluidized by the hot air blowing from the bottom of the regenerator. This fluidized catalyst bed is not a single homogeneous phase and is always very difficult to model due to unclear flow pattern.

For modeling purposes, early researchers divided the fluidization bed into two beds of different densities namely the dense bed and dilute bed. The bottom part of the regenerator consisted of the dense bed wherein most of the catalyst particles were present and the upper part contained dilute bed where mostly gas and fewer catalyst particles were present. Later some more detailed models like grid effect model, two region models and bubbling bed model were developed by various workers. The grid effect model (**Behie and Kehoe, 1973, Errazu et al., 1979**) was developed for the shallow bed with diameter larger than height. In this model it is assumed that air column in the bed are similar in shape and have identical heights and do not intermix with each other. Because of this assumption the simulation of a real process in which this type of grid is not formed leads to serious errors.

A further improvement of the grid effect model came in the form of two regions (**de Lasa and Grace, 1979, de Lasa et al., 1981**). In this model the authors suggested that the dense phase could be further sub-divided into two phases the bubbles phase and emulsion phase. It is assumed that the bubbles in the bubble phases are of same size and do not contain any catalyst particles and the emulsion phase is a mixture of air and catalyst particles and is kept at the minimum fluidization condition.

2.3 Fluid Catalytic Cracking (FCC) Unit Optimization &Control Modes

Several studies have been reported in the open literature dealing with their modeling, simulation, kinetics, multiplicity of steady states, chaotic behavior, on-line optimization and control. **Avidan and Shinnar (1990)** have reviewed the developments in catalytic cracking. The kinetics (**Ancheyta, Lopez, & Aguilar, 1999; Jacob, Gross,**

Voltz, & Weekman, 1976; Weekman, 1969) has been described in terms of different kinetic 'lumps'. These include describing the products in terms of two, three, four, five, ten or twelve lumps, while considering the feed as a single lump. The advantage of ten- and twelve-lump kinetic schemes over the others is that the apparent rate constants are independent of the feed composition, but the main problem is that a relatively large number of kinetic parameters need to be evaluated using experimental or industrial data. These are not easily available. The modeling of the reactor/regenerator system has been studied quite extensively (**Arandes, Azkoiti, Bilbao, & de Lasa, 2000; Arbel, Huang, Rinard, Shinnar, & Sapre, 1995; Dave & Saraf, 2003; De Lasa, Errazu, Barreiro, & Solioz, 1981; Ellis, Li, & Riggs, 1998; Elnashaie & El-Hennawi, 1979; Elnashaie, Abasaeed, & Elshishini, 1995; Elshishini & Elnashaie, 1990; Errazu, de-Lasa, & Sarti, 1979; Han, Chung, & Riggs, 2000; Krishna & Parkin, 1985; Kunii & Levenspiel, 1969).** A detailed review of these several models is provided by **Arbel et al., (1995)** while their strengths and shortcomings have been reviewed critically by **Elshishini and Elnashaie (1990).**

Proper control of the unit allows the refiners to handle changing feed-stocks and market needs. Dynamic models of varying degree of rigor have been proposed by many researchers. The phenomenon of multiplying of steady states makes the control of the unit difficult.

Elshishini et al. (1992) studied the effect of bubble size in reactor and regenerator for all the three steady states. **Elnashaie & Elshishini (1993)** extended their steady state model to an unsteady state model for investigating the dynamic responses of the FCC unit in open-loop and closed-loop feedback controlled modes

Zheng (1994) developed a dynamic model of FCC unit which included the dynamics effects of startup and shutdown. **Arbel et al. (1995)** developed a dynamic model of FCC units which includes more detailed kinetics of the cracking reactions (ten lump schemes) and includes a complete description of CO and CO_2 combustion kinetics incorporating the effect of catalytic combustion promoters in the regenerator.

Ali and Rohani (1997) developed a simple dynamic model of FCC unit. The model does not contain any partial differential equation and is easy to solve and hence can be used particularly for control studies.

Han et al. (2000) developed a detailed dynamic simulator of FCC unit including many auxiliary units (pre-heater, catalyst cooler, blower). They included detailed hydrodynamic of cracking reactor and catalyst regenerator. Their riser model incorporated ten lump cracking reactions scheme and regenerator model incorporated two-regime (dense bed and freeboard) and two phase (emulsion and bubble) behavior of typical fluidized beds

C. Jia et al. (2003) described the FCC unit modeling, identification and model predictive control, a simulation study. Control of the FCC is challenging and there is strong incentive to use multivariable control schemes, such as model predictive control, which accommodate these interactions. The linear multivariables rely on linearized model around the operating point. The authors use a singular algorithm.

Khandalekar and Riggs (1995) applied nonlinear process model based control (PMBC) to model IV industrial problem. They modeled the riser as a plug flow reactor for simplified optimization analysis and applied nonlinear model based control for reactor temperature, regenerator temperature and the flue gas oxygen concentration. They used feed temperature, catalyst circulation rate and regenerator air flow rate as manipulated variables. The dynamic microscopic oxygen and energy balances in the regenerator and the steady state energy balance for the reactor were used as nonlinear models for control.

Sareen and Gupta (1995) had worked on minimization of the reaction time and the cyclic dimer concentration in industrial semibatch nylon 6 reactor for three different grades by using the Sequential Quadratic Programming (SQP).

Mitra et al. (1998) had worked on minimization of the reaction time and the cyclic dimer concentration in industrial semibatch nylon 6 reactor by using the Non-dominated Sorting Genetic Algorithm (NSGA). **Garg and Gupta, 1999** also worked on minimization of total reaction time and the poly-dispersity of the PMMA product by using the Non-dominated Sorting Genetic Algorithm (NSGA). **Rajesh et al. (2000)** describe the minimization of the methane feed rate and maximization of the flowrate of CO in the syngas for a fixed production rate of hydrogen in an existing side-fired steam reformerby using the NSGA. **Bhaskar et al., 2000** describe the minimization of the residence time of the polymer melt and the concentrations of the undesirable side

products formed in the industrial continuous wiped film PET reactor. Equality constraint on the desired degree of polymerization imposed.

Ellis et al. (1998) modeled a type IV FCC unit ten lumps reaction scheme for the reactor. Authors used the steady state optimization models of the regenerator and riser reactor, a simplified reactor yield model, and models of the various process constraints. They also compared the relative performance of constraints control, off-line optimization, and online optimization for different feed characteristics and product pricing structures.

Kasat et al. (2002) described the multi objective optimization of an industrial fluidized bed catalytic cracking unit using Elitist Non dominated Sorting Genetic Algorithm. This genetic algorithm is also use in the determination of kinetic parameters. **Kasat et al. 2003** also describe the multi-objective optimization of an industrial fluidized bed catalytic cracking (FCC) unit using genetic algorithm (GA) with the jumping genes opertaor.

Han et al. (2004) described the process optimization system, which consists of a steady-state process model, a model parameter estimator and a process optimizer for a fluidized catalytic cracking (FCC) process under full and partial combustion modes. First, mathematical modeling was carried out for the reactor, regenerator, main-fractionator, and most of auxiliary units including the feed pre-heater, catalyst cooler, air blower, wet gas compressor, stack gas expander, boilers, and valves. Then, the resulting steady-state model was utilized to develop the model parameter estimator and the process optimizer both of which adopt a successive quadratic programming algorithm to efficiently locate the optimum solutions. The parameter estimator can estimate up to 52 model parameters in order to validate the process model by reducing process–model mismatch. The process optimizer maximizes the economic objective function defined as the difference between the total value of products and the cost of feedstock and utility fewer than 30 operating constraints. The developed optimization system was applied to several optimization cases to maximize the economic profit of the FCC process operated in the full and partial combustion modes and the optimization results were extensively compared and analyzed between the combustion modes.

Chapter-3

Model Formulation

MODEL FORMULATION

A typically FCC unit consists of two reactors, the riser reactor, where almost all the endothermic cracking reactions and coke deposition on the catalyst occur, and the regenerator reactor, where air is used to burn off the accumulated coke. The regeneration process provides, in addition to reactivating the catalyst pellets, the heat required by the endothermic cracking reactions.

The upper fluidized bed immediately above the riser acts as a disengaging chamber where vapor products and heavy components are separated from the catalyst using stripping steam. The only effect of the stripping process is to remove hydrocarbon gases adsorbed inside the pellets before the spent catalyst is sent to the regenerator. The flow rate of the stripping steam is small compared to the flow rates of feed oil and catalyst (the ratio is usually less than 0.25%). Therefore, the effect of steam on the energy balance of the reactor is neglected.

The regenerator is divided into a dense region and the dilute region. The dense region is further divided into two phases: an emulsion phase and a bubble phase. The effect of the dilute region (freeboard region) is not included in the model.

3.1 Riser Reactor Modeling

In the modeling of riser, the hydrodynamics characteristics of riser of a FCC plant are considered the gas and solid velocity profiles by using a plug flow model with radian dispersion. The hydrodynamics proposed by **Pugsley and Berruti (1996) and Gupta and Subba Rao (2001).** Since a large number of complex cracking reactions are involved, calculation of the exact value of the heat of estimate of the heat of reaction may be made by taking the microscopic difference between the enthalpies of the products and the reactants.

For the modeling of the riser reactor, **Ancheyta et al. (1999)** described the five lump kinetic scheme is coupled with the well known material and energy balance equations, in which gas lump is split into dry gas and liquefied petroleum gas (LPG). The model considers five lumps (unconverted gas oil, gasoline, LPG, dry gas and coke)

and it has only nine kinetic constant and one for catalyst deactivation to be estimated. The main advantage of this model over the previous ones is that it can predict the coke formation, which supplies the heat required for the heating and vaporization of the feedstock and to perform the endothermic reactions; LPG, which contains important hydrocarbons (C_3 and C_4) used together with iso-butane as alkylation and MTBE feeds; and dry gas, which is used as fuel gas in refinery. These three products (coke, LPG and dry gas) can be predicted independently from other lumps with the proposed model.

In the model development of riser reactor, the commonly used assumptions are follows below:

1 At the riser inlet hydrocarbon feed comes into contact with the hot catalyst coming from the regenerator and instantly vaporizes (taking latent heat and sensible heat from the hot catalyst). The vapor thus formed move upwards in thermal equilibrium with the catalyst.
2 There is no loss of heat from the riser and the temperature of the reaction mixture (hydrocarbon vapors and catalyst) falls only because of the endothermicity of the cracking reactions.
3 Gas phase velocity variation on account of gas phase temperature and molar expansion due to cracking is considered. Ideal gas law is assumed to hold.
4 Heat and mass transfer resistances are assumed as negligible.
5 There are no radial temperature gradient in the gas and solid phase.
6 Conradson carbon residue of feed is zero.
7 Catalyst deactivation is non-selective and related to coke on catalyst only.
8 Gas oil cracking is a second order reaction but cracking of gasoline and LPG are first order reactions.
9 Dry gas produces no coke.
10 Heat capacities and densities are constant through the length of the reactor.

3.1.1 Riser Kinetics

The cracking reactions are catalyzed by acid sites. The formation of carbonium and carbenium ions and their evolution controls the reaction course. The difficulty comes from the larger number (several thousands) of different molecules. Moreover, each

molecule can potentially take part in a large number of reactions. To complicate the situation further, deactivation occurs rapidly at the same time.

The traditional and global approach of cracking kinetics is lumping. Mathematical models dealing with riser kinetics can be categorized into main types. In one category the lump are made on the basis of boiling range of feed stocks and corresponding products in the reaction system. This kind of models has an increasing trend in the number of lumps of the cracked gas components. The other approach is that in which the lumps are made on the basis of molecular structure characteristics of hydrocarbon group composition in reaction system. This category of models emphasize on more detailed description of the feedstock (**Wang et al. 2005**).

In both of these categories, however, reaction kinetics being considered is that of conversion of lump to another and not the cracking of an individual lump. Theses models do not include chemical data such as type of reaction and reaction stoichiometry. Moreover, the values of kinetics constants depend on the feedstock composition and must be determined for each combination of feedstock and catalyst.

More recently, based upon single event cracking structure oriented lumping and reactions in continuous mixture were proposed by various researchers. Nevertheless, the application of these models to catalytic cracking of industrial feedstocks (vacuum gas oil) is not realized because of the analytical complexities and computational limitations.

In the two main categories of models, it is assumed that when one kg of an individual lump cracks the same amount of another lump is formed with a fixed reaction rate and all rate constants are determined empirically. All these models contradict the basis theme of cracking that when one mole of a reactant cracks down it should give at least two models of products. With this in view, in the present work, a new approach of kinetic scheme is being proposed. The proposed model falls under the first category in which lump are formed on the basis of boiling point, but in this approach, each individual lump is considered as a pure component with known physical-chemical properties. Also the reaction stoichiometry is considered. No separate coke lump is considered and it is assumed that when one mole of a lump crack down is considered and it is assumed that when one mole of a lump cracks down it give one mole each of two other lumps and the balance material gives the coke.

The different lumping models are described, firstly the one lump model was proposed by **Blanding (1953)** treated the kinetic cracking using a one lump conversion model. A study of factors affecting the extent of the reaction is summarized based on the experimental data obtained in developing the fluidized catalytic process. Equations for characterizing the reaction show the rate at constant pressure to be about proportional to the second power of the fraction of the unconverted feed.

Secondly the three lump model was proposed by the **Weekman and Nace (1970).** This model showed a three lump system could be describing gasoline selectivity behavior in catalyst cracking. Subsequent work by Nace et al. (1971) showed that the rate constants for this three lump system changed with charge composition but could be correlated to the paraffin, naphthene and aromatic composition of the charge stock.

Thirdly the four lump model was proposed by **Lee et al. (1989).** This model presents an improved and updated model for modern fluidized bed catalytic cracker, model is different from others mainly in that the deposition rate of coke on catalyst can be predicted from the gas oil conversion and isolated from the C_1-C_4 gas yield. The reactor kinetics to be examines coke formation with conversion and yield of gasoline. The main difference from the three lump model being that coke is independent considered as a lump, other feed, and gasoline and C_1-C_4 gas.

Lastly Advancing the lumping methodology, **Corella and Frances (1991)** developed a 5-lump model, in which the gas-oil lump was divided into its heavy and light fractions. **Dupain et al. (2003)** simplified the 5-lump model of **Corella and Frances (1991)** for the specific case of the catalytic cracking of aromatic gas oil, by reducing the reactions involved in the lumping scheme. Another 5-lump model was developed by **Larocca et al. (1990)**, in which the **3-lump model of Weekman** was modified by splitting the gas oil lump into aromatic, paraffinic, and naphthtenic lumps. **Ancheyta et al. (1999)** followed a different approach in their 5-lump models development, in which they considered the gas oil as one lump, but divided the gas lump into two lumps (liquefied product gas and dry gas).

The atmospheric residuum increases the amount of coke and gaseous products, particularly hydrogen content in dry gas, from the dehydrogenation activity of nickel and vanadium, causing limitations in the plant operation in terms of gas compression or

regeneration air blowing capacity, in addition to the negative effect on gasoline yield and catalyst deactivation. Thus, the prediction of dry gas and coke yields becomes very important to design and simulate the gas compressor and air blower.

One limitation is that the kinetic model does not consider products heavier than gas oil, such as light cycle oil and heavy cycle oil. These two products are taken together as the unconverted gas oil in the proposed model. Another limitation is that the parameters of the kinetic model depend on the feedstock and catalyst properties.

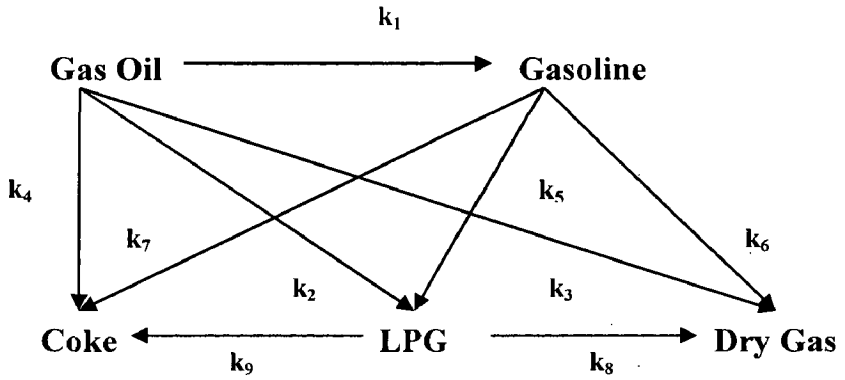

Figure 3.1: Schematic diagram of the five-lump model examined.

The present kinetic scheme is differ from that used by Ancheyta et al. (1999) in that the latter did not allow cracking of gasoline and LPG to coke which have been included in the present study. So in the present kinetic model, nine kinetic constant are estimated by experimental and theoretically approach. The model parameters are estimated by minimizing the error between the data obtained from the steady state process model and those from the hypothetical process model.

Gas oil: $(r_1) = -(k_1 + k_2 + k_3 + k_4) y_1^2 \phi$ (3.1)

Gasoline: $(r_2) = (k_2 y_1^2 - k_5 y_2 - k_6 y_2 - k_7 y_2)\phi$ (3.2)

LPG: $(r_3) = (k_2 y_1^2 + k_5 y_2 - k_8 y_3 - k_9 y_3)\phi$ (3.3)

Dry gas: $(r_4) = (k_3 y_1^2 + k_6 y_2 + k_8 y_3)\phi$ (3.4)

Coke: $(r_5) = (k_4 y_1^2 + k_7 y_2 + k_9 y_3)\phi$ (3.5)

The riser modeled as vertical tube comprising of a number of equal sized compartments (or volume elements) of circular cross section (Figure: 3.2). Volume elements are designed by symbol j (j = 1, 2, 3 ...., N_c) and numbering of the volume elements is done from bottom (inlet) to top (outlet). Each volume element is assumed to contain two phases (i) solid phase (catalyst and coke) and (ii) gas phase (vapors of feed and product hydrocarbon and steam). In a volume element, each phase is assumed to be well mixed so that heat and mass transfer resistances can be ignored. Model equation are written for both the phases in each j^{th} volume element for all pseudocomponents PC_i (i= 1, 2 ...N). Cracking reactions rate constants in each volume element are evaluated at the local temperature of the j^{th} volume element and are subsequently used for calculating the change in molar concentration of each component and the heat of reactions.

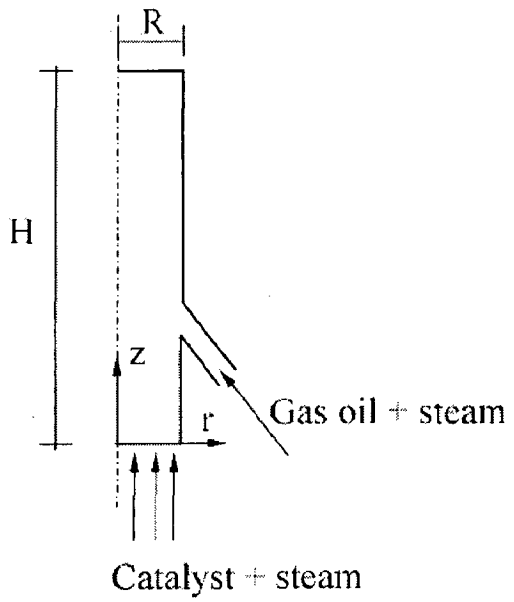

Figure 3.2: Schematic diagram of feed injection in FCC riser

Balances: On the basis of above assumption, the mole balance for the j^{th} lump over a differential element can be written as follows

$$\frac{dF_j}{dh} = A_{ris} H_{ris} (1 - \varepsilon) \rho_c \sum_{i=1}^{9} \alpha_{ij} r_i \qquad j = 1, 2, ...5 \qquad (3.6)$$

Where j = 1 to 5 represents gas oil, gasoline, LPG, dry gas, and coke respectively. i = 1 to 9 represents the reactions as shown in figure: 3.1

$$MW_g = \sum_{j=1}^{5} x_j MW_j \tag{3.7}$$

$$\rho_v = \frac{P_{ris}\, MW_g}{RT} \tag{3.8}$$

$$\varepsilon = \frac{\dfrac{F_{feed}}{\rho_v}}{\dfrac{F_{feed}}{\rho_v} + \dfrac{F_{rgc}}{\rho_c}} \tag{3.9}$$

$$\alpha_{ij} = \frac{MW_i}{MW_j} \tag{3.10}$$

Table: 3.1 Kinetic and Thermodynamic Parameters used for the Reactor Modeling (obtained from the Kasat et al. 2002)

Rate Constant	Reaction	Frequency Factor	Activation Energy (kJ/kmol)	Heat of Reaction (kJ/kmol)
k1	Gas Oil to Gasoline	19584.55*	57540	45000
k2	Gas Oil to LPG	3246.45*	52500	159315
k3	Gas Oil to Dry Gas	559.90*	49560	159315
k4	Gas Oil to Coke	41.44*	31920	159315
k5	Gasoline to LPG	65.40	73500	42420
k6	Gasoline to Dry Gas	0.00	45360	42420
k7	Gasoline to Coke	0.00	66780	42420
k8	LPG to Dry Gas	0.32	39900	2100#
k9	LPG to Coke	0.19	31500#	2100#

* Values determined from the plant data by regression (m^6/ (kg catalyst) (kmol gas oil) (s) for the reactions 1 to 4, (m^3/ (kg catalyst) (s) for reactions 5 to 9

Estimated

Table 3.2: Kinetic Parameters used for Regenerator Modeling (Obtained from the Arbel et al. (1995))

Kinetic Parameter	Frequency Factor	Activation energy (E/R, K)
β_c	2512	6795
K_c (1/(atm)(s))	1.069×10^{8}	18890
K_{3c} ((kmol CO)/ (kg cat.)(s) (m^3))	117	13890
K_{3h} ((kmol CO)/ (m^3) $(atm)^2$ (s)	5.07×10^{14}	35555

The molecular weights of different lumps used for the calculation of α_{ij} are given in table: 3.3. The rate equation in (kmol)/ (kg cat.) (s) are given by following expressions:

$$r_i = k_{0,i} \exp(-\frac{E}{RT}) C_1^{\,2} \phi \qquad \text{for i = 1,2,3,4} \qquad (3.11)$$

$$r_i = k_{0,i} \exp(-\frac{E}{RT}) C_2 \phi \qquad \text{for i = 5,6,7} \qquad (3.12)$$

$$r_i = k_{0,i} \exp(-\frac{E}{RT}) C_3 \phi \qquad \text{for i = 8,9} \qquad (3.13)$$

Where, C_1, C_2 and C_3 are concentration of gas oil, gasoline and LPG respectively.

Table: 3.3 Thermodynamics and other Parameters used for Simulation (obtained from the Kasat et al. 2002)

Parameter	Numerical Value
$C_{P,c}$ (kJ/kg K)	1.003
$C_{P,fl}$ (kJ/kg K)	3.430
$C_{P,fv}$ (kJ/kg K)	3.390
$C_{P,N2}$ (kJ/kg K)	30.530
$C_{P,O2}$ (kJ/kg K)	32.280
$C_{P,H2O}$ (kJ/kg K)	36.932
$C_{P,CO}$ (kJ/kg K)	30.850

$C_{P,CO2}$ (kJ/kg K)	47.400
ΔH_{evp} (kJ/kg)	350.0
H_{CO} (kJ/kg)	1.078×10^{5}
H_{CO2} (kJ/kg)	3.933×10^{5}
H_{H2O} (kJ/kg)	2.42×10^{5}
X_{Pt}	0.10
ρ_c (kg/m^3)	1089.0
C_H (kg H_2/kg coke)	0.165
D_P (ft)	2.0×10^{-4}
$MW_{gas\ oil}$	350
$MW_{gasoline}$	114
MW_{LPG}	52
$MW_{dry\ gas}$	30
MW_{coke}	12
Gas oil lump Boiling range °C	›221
Gasoline lump Boiling range °C	30-220

For the modeling of the catalyst deactivation, the function proposed by **Yingxun (1991)** for the catalytic cracking of vacuum gas oil was used. Thus, the function ϕ was related to coke on catalyst as follows:

$$\phi = (1 + 51C_c)^{-2.78} \tag{3.14}$$

Due to the endothermic cracking reactions in the riser, there is a temperature drop along the height of the riser. The enthalpy balance across a differential element of height dh of the riser can be represented as follows:

$$\frac{dT}{dh} = \frac{A_{ris} H_{ris} (1-\varepsilon)\rho_c}{F_{rgc} C_{P_C} + F_{feed} C_{P_{fv}}} \sum_{i=1}^{9} r_i (-\Delta H_i) \tag{3.15}$$

The regenerated catalyst and the preheated feed are mix at the base of the riser. Temperature at this zone can be determined from enthalpy balance. Assuming a 10°C drop in temperature of the regenerated catalyst during its journey in transfer line, the riser bottom temperature is calculated as follows:

$$T(h=0)=\frac{F_{rgc}C_{P_c}(T_{rgn}-10)+F_{feed}C_{P_{fl}}T_{feed}-\Delta H_{evp}F_{feed}-Q_{loss,ris}}{F_{rgc}C_{P_c}+F_{feed}C_{P_{fv}}} \quad (3.16)$$

where,

$$Q_{loss,ris} = 0.019\ [F_{rgc}C_{p_c}(T_{rgn}-10)+F_{feed}C_{P_{fl}}T_{feed}-\Delta H_{evp}F_{feed}]$$

To match the riser base temperature with the plant value, so the empirical term $Q_{loss, ris}$ can be incorporated.

3.2 Stripper Modeling

Due to the lack of required design and operating data the performance of the stripper has been idealized. The temperature drop across the industrial stripper was observed to be 8-12°C. So the temperature drop across the stripper was assumed to be 10°C by **Dave and Saraf (2002)** and 13.88°C by **Arbel et al. (1995)**.

The temperature of the spent catalyst entering the regenerator is calculated by following equation:

$$T_{sc}=T_{ris,top}-\Delta T_{st} \quad (3.17)$$

3.3 Regenerator Modeling

The primary objective of the regenerator is to burn off coke deposition on the spent catalyst to restore catalyst activity. There are two types of regenerators in FCC operation; one operates in the partial combustion mode and the other in the total combustion mode. In partial combustion mode, a less than theoretical, or stoichiometric, amount of air is provided to the regenerator. Only part of the carbon in coke is reacted to carbon dioxide and the remainder of the carbon is reacted to carbon monoxide. Ideally, all oxygen should be consumed and no oxygen should be present in the flue gas. In the total combustion mode, excess air is provided to the regenerator. Ideally, the entire carbon component in the coke should be reacted to carbon dioxide and no carbon monoxide should be present in the flue gas.

The regenerator was described by the two region model, proposed by the **Krishna and Perkins (1985)** with some modification. The first region is dense bed of the regenerator in which bulk of the overall coke combustion takes place. The second region

in the model is the dilute phase above the dense bed, afterburning of carbon mono-oxide and catalyst entrainment are important effects of this section. In this dilute phase section, the gas stream carries some catalyst particle. The rate of the solids entrainment is usually very small compared to the total amount of catalyst retained in the regenerator vessel. Most of the coke on the catalyst pellets has already been combusted in the dense region.

The development of the steady state model is based on the following assumptions:

1. Gas is in the plug flow throughout the bed and in thermal equilibrium with surrounding bed.
2. Catalyst in dense bed is well mixed and isothermal with uniform carbon on the catalyst particles.
3. Kinetics of the coke combustion assumes catalyst particles to be 60 μm sizes.
4. Resistance to mass transfer from gas to catalyst phase is negligible.
5. Mean heat capacities of gases and catalyst are assumed to remain constant over the temperature range encountered.
6. All entrained catalyst is returned via cyclones.

3.3.1 **Regenerator Kinetics**

The following combustion reactions are considered to be taking place in the regenerator.

1. $C+\frac{1}{2}O_2 \xrightarrow{k_1} CO$ (3.18)
2. $C+O_2 \xrightarrow{k_2} CO_2$ (3.19)
3. $CO+\frac{1}{2}O_2 \xrightarrow{k_{3c}} CO_2$ (Heterogeneous CO combustion) (3.20)
4. $CO+\frac{1}{2}O_2 \xrightarrow{k_{3h}} CO_2$ (Homogeneous CO combustion) (3.21)
5. $H_2+\frac{1}{2}O_2 \xrightarrow{k_4} H_2O$ (3.22)

The coke combustion in the reaction (3.13) and (3.14) are proportional to C_{rgc} and partial pressure of O_2 in the regenerator (P_{O2}). The CO combustion reactions (3.15) and

(3.16) are proportional to P_{O2} and partial pressure of CO in the regenerator (P_{co}). The rate expressions for these reactions are:

Rate of reaction 1

$$r_1 = (1 - \varepsilon)\rho_{cat} k_1 \frac{C_{rgc} f_{O_2}}{MW_{coke} f_{Tot}} P_{rgn} \quad (3.23)$$

Rate of reaction 2

$$r_2 = (1 - \varepsilon)\rho_{cat} k_2 \frac{C_{rgc} f_{O_2}}{MW_{coke} f_{Tot}} P_{rgn} \quad (3.24)$$

Rate of reactions 3

$$r_3 = (x_{Pt} (1 - \varepsilon)\rho_{cat} k_{3c} + \varepsilon k_{3h}) \frac{f_{O_2} f_{CO}}{f_{Tot}^2} P_{rgn}^2 \quad (3.25)$$

Where, x_{Pt} is a relative catalytic CO combustion rate.

The initial ratio of CO/CO_2 at the catalyst surface given by **Weisz (1966)** is

$$\left(\frac{CO}{CO_2}\right)_{surface} = \frac{k_1}{k_2} = \beta_c = \beta_{c0} \exp\left(\frac{-E_\beta}{RT}\right) \quad (3.26)$$

If k_c is overall coke combustion rate then

$$k_c = k_1 + k_2 = k_{c0} \exp\left(\frac{-E_c}{RT}\right) \quad (3.27)$$

Where,

$$k_1 = \frac{\beta_c k_c}{\beta_c + 1} = \frac{\beta_c k_{c0} \exp\left(\frac{-E_c}{RT}\right)}{\beta_c + 1} \quad (3.28)$$

$$k_2 = \frac{k_c}{\beta_c + 1} = \frac{k_{c0} \exp\left(-\frac{E_c}{RT}\right)}{\beta_c + 1} \quad (3.29)$$

From the above equations, the overall rate of the reaction of O_2, CO, and CO_2 in j^{th} compartment can be written as

$$r_{O_2} = (1 - \varepsilon)\rho_{cat} \left(\frac{k_1}{2} + k_2\right) \frac{C_{rgc} f_{O_2,j-1}}{MW_{coke} f_{Tot}} P_{rgn} V_j + \frac{k_3 f_{O_2} f_{CO}}{2 f_{Tot} f_{Tot}} p_{rgn}^2 V_j \quad (3.30)$$

$$r_{CO} = (1-\varepsilon)\rho_{cat} k_1 \frac{C_{rgc} f_{O2,j-1}}{MW_{coke} f_{Tot}} P_{rgn} V_j - k_3 \frac{f_{O2} f_{CO}}{f_{Tot} f_{Tot}} P_{rgn}^2 V_j \quad (3.31)$$

$$r_{CO2} = (1-\varepsilon)\rho_{cat} k_2 \frac{C_{rgc} f_{O2,j-1}}{MW_{coke} f_{Tot}} P_{rgn} V_j + k_3 \frac{f_{O2} f_{CO}}{f_{Tot} f_{Tot}} P_{rgn}^2 V_j \quad (3.32)$$

3.3.2 **Dense Bed Modeling**

The spent catalyst from the reactor enters the regenerator dense bed in which coke is burntoff in the presence of air to CO, CO_2 and H_2O. The oxidation of hydrogen is assumed to be instantaneous and complete and hence the amount of oxygen available for the carbon burning reactions at the dense bed inlet is that remaining after the hydrogen combustion reaction.

Differential Balances:

Material and energy balance across a differential element of height dz of the dense bed are as follows:

Material Balance:

$$\frac{df_{O2}}{dz} = -A_{rgn}\left(\frac{r_1}{2} + r_2 + \frac{r_3}{2}\right) \quad (3.33)$$

$$\frac{df_{CO}}{dz} = -A_{rgn}(r_3 - r_1) \quad (3.34)$$

$$\frac{df_{CO2}}{dz} = -A_{rgn}(r_2 + r_3) \quad (3.35)$$

Energy Balance:

$$\frac{dT}{dz} = 0 \quad (3.36)$$

Initial Conditions:

$$f_{H_2O} = F_{rgc}(C_{sc} - C_{rgc})\frac{C_H}{MW_H} \quad (3.37)$$

$$f_{O_2}(0) = 0.21 F_{air} - \frac{1}{2} f_{H_2O} \quad (3.38)$$

$$f_{CO}(0) = f_{CO_2}(0) = 0 \quad (3.39)$$

$$f_{N_2} = 0.79\ F_{air} \tag{3.40}$$

Total gas flow rate at any cross section is given by:

$$f_{Tot} = f_{H_2O} + f_{O_2} + f_{CO} + f_{CO_2} + f_{N_2} \tag{3.41}$$

Bed Characteristics:

Gas molar density (kmol/m^3)

$$\rho_g = \frac{P_{rgn}}{RT_{rgn}} \tag{3.42}$$

Superficial linear gas velocity (m/s)

$$u = \frac{F_{air}}{\rho_g A_{rgn}} \tag{3.43}$$

Void fraction was calculated using the correlations reported by **Ewell and Gadmer (1978)**:

$$\varepsilon = \frac{0.305\ u_1 + 1}{0.305\ u_1 + 2} \tag{3.44}$$

Where, u_1 = superficial linear velocity in ft/s.

Dense bed height is also calculated using the correlation reported by **Ewell and Gadmer (1978)**:

$$Z_{bed} = 0.3048\ (TDH) \tag{3.45}$$

$$TDH = TDH_{20} + 0.1(D - 20) \tag{3.46}$$

$$Log_{10}(TDH_{20}) = \log_{10}(20.5) + 0.07(u_1 - 3) \tag{3.47}$$

Where, D is the regenerator diameter in ft, TDH means transport disengaging height.

The volume of a compartment jth in the regenerator dense bed is given by:

$$V_j = A_{rgn}\ \Delta z_j \tag{3.48}$$

Where, $\Delta z_j = \frac{H_{densebed}}{N_c}$

Overall Balances:

Carbon balance for the regenerator in the dense bed:

$$C_{rgc} = \frac{F_{sc} C_{sc} (1 - C_H) - (f_{CO\,(Zbed)} + f_{CO_2(Zbed)}) MW_c}{F_{rgc} (1 - C_H)} \tag{3.49}$$

Heat Balance:

Applying heat balance across the regenerator dense bed gives the expression for the dense bed temperature:

$$T_{rgn} = T_{base} + \left\{ \frac{\begin{array}{c} f_{CO\,(Zbed)} H_{CO} + f_{CO_2(Zbed)} H_{CO_2} + f_{H_2O} H_{H_2O} + \\ F_{air} C_{P_{air}} (T_{air} - T_{base}) + F_{sc} C_{P_c} (T_{sc} - T_{base}) - Q_{loss,rgn} \end{array}}{\begin{array}{c} F_{rgc} C_{P_c} + f_{CO_2(Zbed)} C_{P_{CO_2}} + f_{CO\,(Zbed)} C_{P_{co}} + \\ f_{O_2} C_{P_{O_2}} + f_{H_2O} C_{P_{H_2O}} + f_{N_2} C_{P_{N_2}} \end{array}} \right\} \tag{3.50}$$

3.3.3 **Dilute Phase Modeling**

Plug flow kinetics is assumed in the dilute phase. The main reaction taking place in the dilute phase is the oxidation of CO to CO_2. As a result both carbon concentration and temperature varies as a function of height in the dilute phase. Material and energy balance in the dilute phase results in the following equation.

Material Balance:

$$\frac{df_{O_2}}{dz} = -A_{rgn} \left(\frac{r_1}{2} + r_2 + \frac{r_3}{2}\right) \tag{3.51}$$

$$\frac{df_{CO}}{dz} = -A_{rgn} (r_3 - r_1) \tag{3.52}$$

$$\frac{df_{CO_2}}{dz} = -A_{rgn} (r_2 + r_3) \tag{3.53}$$

$$\frac{df_c}{dz} = -A_{rgn} (r_1 + r_2) \tag{3.54}$$

Energy Balance:

$$\frac{dT_{dil}}{dz} = \frac{1}{f_{Tot} C_{P,Tot}} \left(H_{co} \frac{df_{CO}}{dz} + H_{CO_2} \frac{df_{CO_2}}{dz}\right) \tag{3.55}$$

Where,

$$C_{P,Tot} = \left(\frac{C_{P_{N_2}} f_{N_2} + C_{P_{O_2}} f_{O_2} + C_{P_{CO}} f_{CO} + C_{P_{CO_2}} f_{CO_2} + C_{P_{H_2O}} + C_{P_c} F_{ent}}{f_{Tot}} \right)$$

Entrainment is calculated by using the correlation of **Ewell and Gadner (1978)**:

$$Y = \frac{W}{V \rho_f} \tag{3.56}$$

$$X = \frac{V^2}{g D_p \rho_p^2} \tag{3.57}$$

$$Log_{10} Y = \log_{10} 60 + 0.69 \log_{10} X - 0.445 (\log_{10} X)^2 \tag{3.58}$$

$$F'_{ent} = WA_{rgn} \tag{3.59}$$

$$F_{ent} = 0.4535 \ (F'_{ent}) \tag{3.60}$$

Catalyst density and void fraction in the dilute phase:

$$\rho_{dil} = \frac{F_{ent}}{A_{rgn} u_{rgn}} \tag{3.61}$$

$$\varepsilon = 1 - \frac{\rho_{dil}}{\rho_c} \tag{3.62}$$

The initial flow rate of coke in the dilute phase is given by:

$$f_c(0) = F_{ent} C_{rgc} \frac{(1 - C_H)}{12} \tag{3.63}$$

The height of dilute phase is calculated from the following expression:

$$Z_{dil} = Z_{rgn} = Z_{bed}$$

3.4 Solution Procedure

In the present work, some important points have been discussed. These points have been considered for the solution of five lump kinetic schemes, in which the feed is considered as vacuum gas oil and the products lumps are gasoline, LPG, dry gas and coke.

1. The initial values of coke on regenerated catalyst (C_{rgc}) and regenerator temperature (T_{rgn}) is assumed.
2. Rate equations of all the five lumps are integrated along the riser length with a small step size using **Runga Kutta** method and subsequently coke on spent catalyst (C_{sc}) and riser top temperature ($T_{ris,top}$) is calculated.
3. Then the dense bed calculations are carried out to obtain calculated values of carbon on regenerated catalyst (C_{rgc}) and dense bed temperature (T_{rgn}).
4. Rate equations in the dilute phase bed are also integrated to obtain flue gas composition and temperature.
5. If the calculated values of (C_{rgc}) and (T_{rgn}) do not match with the assumed values then repeat the calculations with the calculated values as the new assumed values.
6. Gas oil conversion, product yields in the reactor and flue gas composition and temperature are evaluated at the converged values of (C_{rgc}) and (T_{rgn}).

The model equation for the riser and the regenerator modules are written in MATLAB and the corresponding non-linear equations are solved using MATLAB only. Convergence is obtained iterative method. Tolerance of 1°C for (T_{rgn}) and 5×10^{5} kg coke/kg catalyst for (C_{rgc}) are used. Table: 4 shows the design data of the FCC unit used in this study and solving this model.

Table: 3.4 Design data for the FCC unit (Dave and Saraf, 2003)

Parameter	**Value**
Riser length (m)	37.0
Riser diameter (m)	0.68
Regenerator length (m)	19.34
Regenerator diameter (m)	4.52
Catalyst hold up in the regenerator (vol %)	40.5

3.5 Introduction of Genetic Algorithm

Till the last decade, most of the problems solved in the field of optimization involved only a single objective function. The thrust towards solving more complex, real-

life problems has led to encounters with multiple objectives and to the development of more efficient, multiple-objective optimization techniques. Vector-evaluated GA (**Schaffer, 1984**), vector-optimized evolution strategy (**Kursawe, 1990**), weight-based GA (**Hajela et al., 1992**), random-weighted GA (**Murata, 1997**), NSGA (**Srinivas & Deb, 1994**), multiple-objective GA (**Fonseca & Fleming, 1993**), and niched Pareto GA (**Horn & Nafploitis, 1993**), are a few examples.

A few examples of algorithms incorporating the concept of elitism are the elitist multi-objective evolutionary algorithm (**Rudolph, 2001**), the elitist NSGA-II (**Deb et al., 2002**), distance-based Pareto GA (**Osyczka & Kundu, 1995**), strength Pareto evolutionary algorithm (**Zitzler & Thiele, 1998**), thermodynamical GA (**Kita, Yabumoto et al., 1996**), Paretoarchived evolution strategy (**PAES; Knowles & Corne, 2000**), and multi-objective messy GA (**van Veldhuizen, 1999**).

It was inferred that none of the optimization techniques is perfect and that there is always room for improvement. Hence, a continuous search is always on for faster algorithms, or algorithms that have better convergence characteristics. The concept of JG or transposons in natural genetics find that this adaptation obtains solutions for the multi-objective optimization of FCC units in almost one-fifth of the CPU time (number of generations) as compared to that taken by NSGA-II.

3.5.1 Jumping Genes (JG)

Since the algorithm NSGA-II-JG developed by **Stryer (2000)**, in the 1940s, **McKlintock (1987)** predicted the existence of JG, a DNA that could jump in and out of chromosomes. Initially, scientists considered DNA as stable and invariable, and so the idea of JG met with considerable cynicism. But in the late 1960s, scientists succeeded in isolating JG from the bacterium, Escherichia coli, and named these as transposons. In the 1970s, the role of transposons in transferring bacterial resistance to antibodies became understood, and led to increased interest in their study. At the same time, it was found that transposons also generated genetic variation (diversity) in natural populations. It was observed that these extra-chromosomal transposons were not essential for normal life, but could confer on it properties such as drug resistance and toxigenicity, and, under appropriate conditions, offer advantages in terms of survival.

Transposons, having a relatively small size of about 1-2 kb (kilo-bases or kilo-nucleotides), can get inserted (replace a sequence of the same length) in a (original) chromosome. These are referred to as insertion sequences. These consist of a central coding sequence of bases that is flanked on both sides by short, inverted, repeat sequences (Figure 3.3).

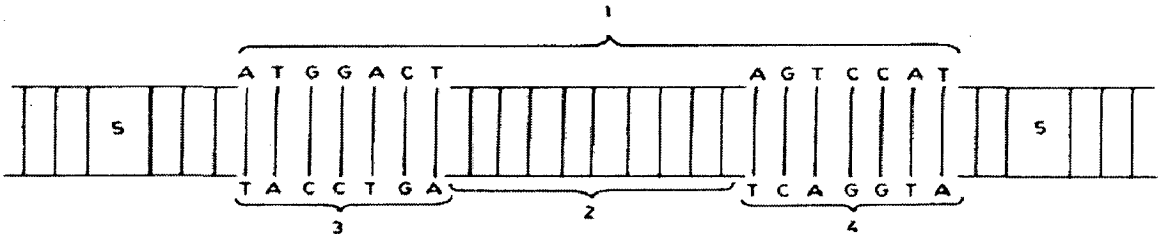

Figure 3.3: Schematic representation of a transposon. (1) Transposon inserted in a chromosome; (2) Genes in the transposon; (3 and 4) Inverted repeat sequences of bases/nucleotides; (5) Double-stranded DNA of original chromosome. Bases: A, adenine; C, cytosine; G, guanine; T, thymine.

Transposons can also be of larger sizes of approximately 4-25 kb, and may carry a variety of resistance and other genes, with long repeat sequences at either end. Some transposons have unique sites (short, specific sequences of DNA) that act as a forwarding address, directing the transposon to a complementary DNA site in the host genome. Usually, there are multiple copies of such appropriate sites in the host genome. Hence, a transposon can get attached to any of these sites randomly. Indeed, transposons can move (jump) from site to site on the same or on a different DNA molecule, a process referred to as transposition. The enzymes produced by the transposons provide the physical mechanism for the jump on to a host. It is clear that besides the introduction of new information, the insertion of transposons disturbs the sequence of chromosomal DNA causing deletion, duplication, inversion or other alterations.

3.5.2 Non-dominated Sorting Genetic Algorithm (NSGA)-II-JG

The two kinds of JG to adapt the binary-coded, elitist NSGA-II (**Deb, 2001; Deb et al., 2002**). The two adaptations used in this study are shown in Figure 3.4.

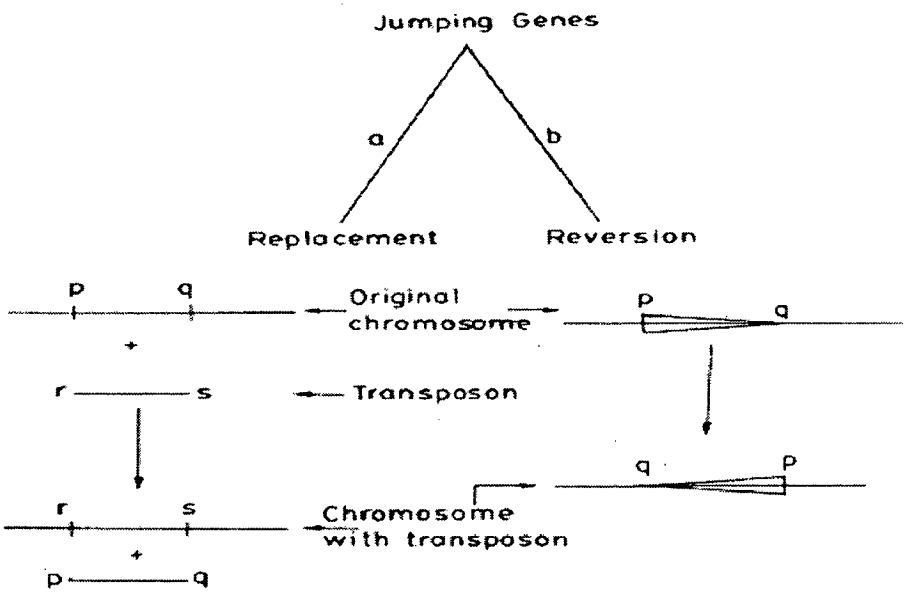

Figure 3.4: schematically diagram of two adaptations of JG in GA.

These mimic natural genetics to a large extent, a probabilistic approach is used. A fraction, P jump, of strings (selected randomly) in the population, are modified by the 'jumping gene' operator (either a or b in Figure 3.4). In the case of replacement, a part of the binary string in the offspring population is replaced with a newly (randomly) generated binary string having the same length. The jumping string is generated using random numbers, using the same procedure as used for generating members of the initial population. The two sites (p and q in Figure 3.4, path a) in the original chromosome, between which replacement occurs, are selected using random numbers. In case of reversion, the binaries between two sites, p and q (in Figure 3.4, path b) selected using random numbers, in a chromosome in the offspring population, are reversed.

3.6 Problem Formulation

We have presented solutions of four multi-objective optimization problems (three problems involving two objective functions, and one with three objectives) for an industrial FCCU, using NSGA-II

Max f1 (Tfeed, Tair, Fcat, Fair) = gasoline yield

Min f2 (Tfeed; Tair; Fcat; Fair) = %coke

Subject to

$700 \leq T_{rgn} \leq 950$ K

The two objective functions are the maximization of the yield of gasoline (economic reasons) and the minimization of the coke formed on the catalyst during the cracking of heavy compounds (to minimize catalyst decay and so to reduce the production of CO). The decision variables used are the feed preheat temperature (Tfeed), the air preheat temperature (Tair), the catalyst flow rate (Fcat), and the air flow rate (Fair). A constraint is put on the temperature of the regenerated catalyst (Trgn).

Table 3.5: GA parameters and bounds used in optimization

Parameter	Value
N_P	100
P_{cross}	0.95
P_{mut}	0.05
P_{jump}	0.5
$N_{gen,max}$	50
l_{chr}	40
N_{seed}	0.88876
n	4
Bounds	$575 \leq T_{feed} \leq 670$ K
	$450 \leq T_{air} \leq 525$ K
	$115 \leq F_{cat} \leq 290$ kg/s
	$11 \leq F_{air} \leq 46$ kg/s

3.7 Solution Technique

The lower coke formation in the present study is considered for similar values of the gasoline yield. This is expected since we are minimizing the coke formation explicitly here. Clearly, minimizing the coke formation in the riser does not, necessarily, lead to lower CO concentrations in the flue gas coming out of the regenerator (obviously, the optimal values of the decision variables are different for the two cases). The importance of solving optimization problems with several objective functions is brought out by this comparison. We may add that the five two- and three objective optimization problems

solved for the industrial FCC unit provide a good variety to a decision maker, who can choose the results relevant to him, or generate newer results using the NSGA-II-JG adaptation suggested herein.

It may be mentioned at the end that optimization techniques (like GA) that are stochastic in nature, offer advantages over popular classical optimization techniques, e.g., sequential quadratic programming (SQP) used along with the one-constraint method (**Chankong & Haimes, 1983**) to obtain Paretos. The latter require good initial guesses, are not nearly as robust as those belonging to the first category, and are extremely cumbersome to use if we have more that two objective functions. **Bhaskar et al. (2000)** have mentioned that GA and its adaptations are extremely robust and (when they do converge, and that happens quite often) give the entire Pareto set in a single application.

The Jumping Genes (JG) operator is speeding up the computational for obtaining solutions of multi-objective optimization problems. The elitist non-dominated sorting genetic algorithm with jumping genes, (NSGA-II-JG) can be used to solve this problem (Appendix-II).This algorithm have been successfully solve the optimization problem with much faster speed up as compared to NSGA (**Kasat et al. 2002**).

Chapter-4

Result & Discussion

RESULT & DISCUSSION

4.1 Solution of Modeling Equation

Most of the model involves the gaseous products as a lump and in some cases the gases are also lumped together with the coke yield. The prediction of coke yield separately from other lumps becomes very important to perform heat integration studies and to design and simulate air blowers and the FCC reactor and regenerator. In the present work, the 5-lump kinetic model for catalytic cracking which splits the light gas oil into dry gas and LPG. This separation is very important because the key FCC products can be predicted separately.

In the FCC unit, there are the riser reactor, stripper and regenerator modeling equations. These ordinary differential equations can be solved by the Runga Kutta method with the help of MATLAB. MATLAB is a high performance language for technical computing. It integrates computation, visualization, and programming in an easy to use environment where problems and solutions are expressed in familiar mathematical notation.

Table 4.1 shows a comparison of model predicted yields with the measured values for two data sets. The first seven rows of the table are required by the simulator as inputs. The match between the model predicted yields and the measured data is reasonably good. The performance of the model can be expected to remain the same as long as the feed composition remains the same.

Table 4 .1: Comparison of the model predicted parameters with the plant value

Type	Set 1		Set 2	
	Measured	**Predicted**	**Measured**	**Predicted**
Feed flow rate (kg/s)	31.47	-	32.11	-
Feed preheat temperature (K)	617.4	-	620.7	-
Catalyst flow rate (kg/s)	208.33	-	205.00	-
Riser pressure (atm)	2.457	-	2.506	-
Air flow rate (kmol/s)	0.56	-	0.571	-

Air preheat temperature (K)	490.3	-	493.3	-
Regenerator pressure (atm)	2.588	-	2.638	-
Riser top temperature (K)	765.5	774.68	766.6	778.21
Regenerator temperature (K)	930.2	939.51	934.6	948.57
Gas oil (%)	48.1	51.858	44.1	52.815
Gasoline (%)	32.6	32.797	35.2	33.387
LPG (%)	12.1	11.912	12.6	12.093
Dry gas (%)	3.1	3.2749	3.8	3.3187
Coke (%)	4.1	3.772	4.3	3.783
Dense bed height (m)	-	6.514	-	6.5567
Coke on regenerated catalyst (%)	-	0.56726	-	0.54841
Entrained catalyst flow rate (kg/s)	-	32.609	-	32.609

Figure 4.1 shows the progress of cracking along the riser /reactor length while figure 4.2 shows the same against the residence time in the riser/reactor. Initially the conversion and hence, the product yields, increase sharply along the riser height but this rate temperature tapers off as we move up along the reactor length.

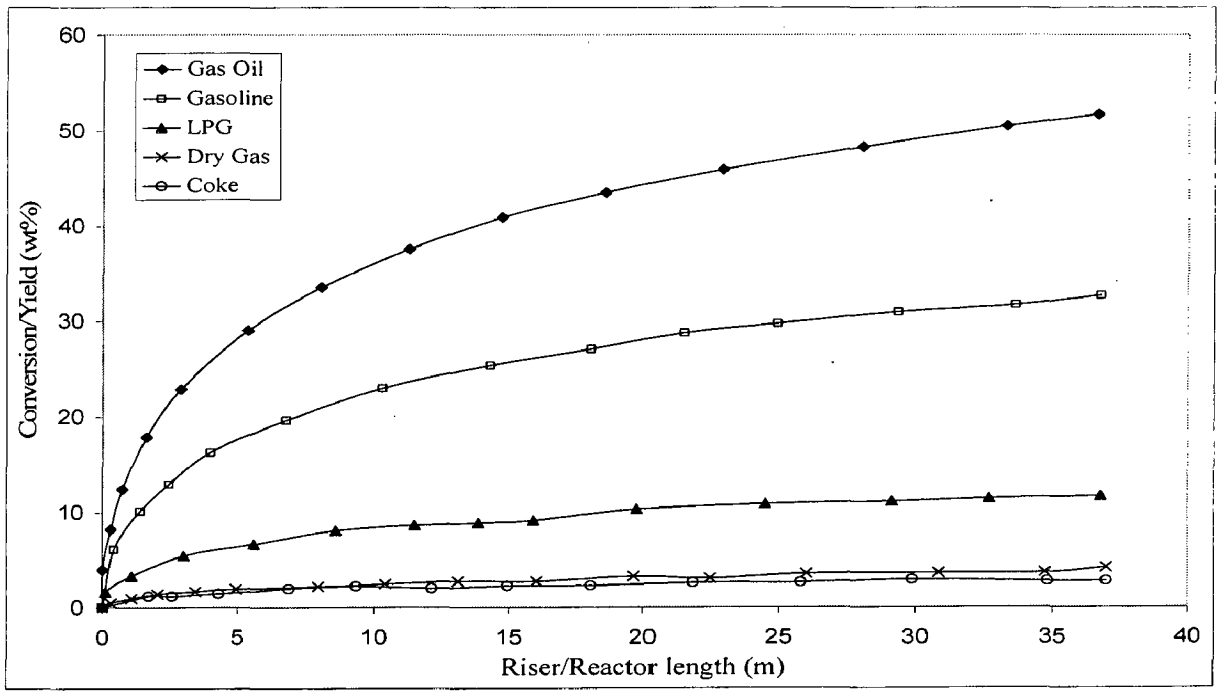

Figure 4.1: Product profile along the riser/reactor height

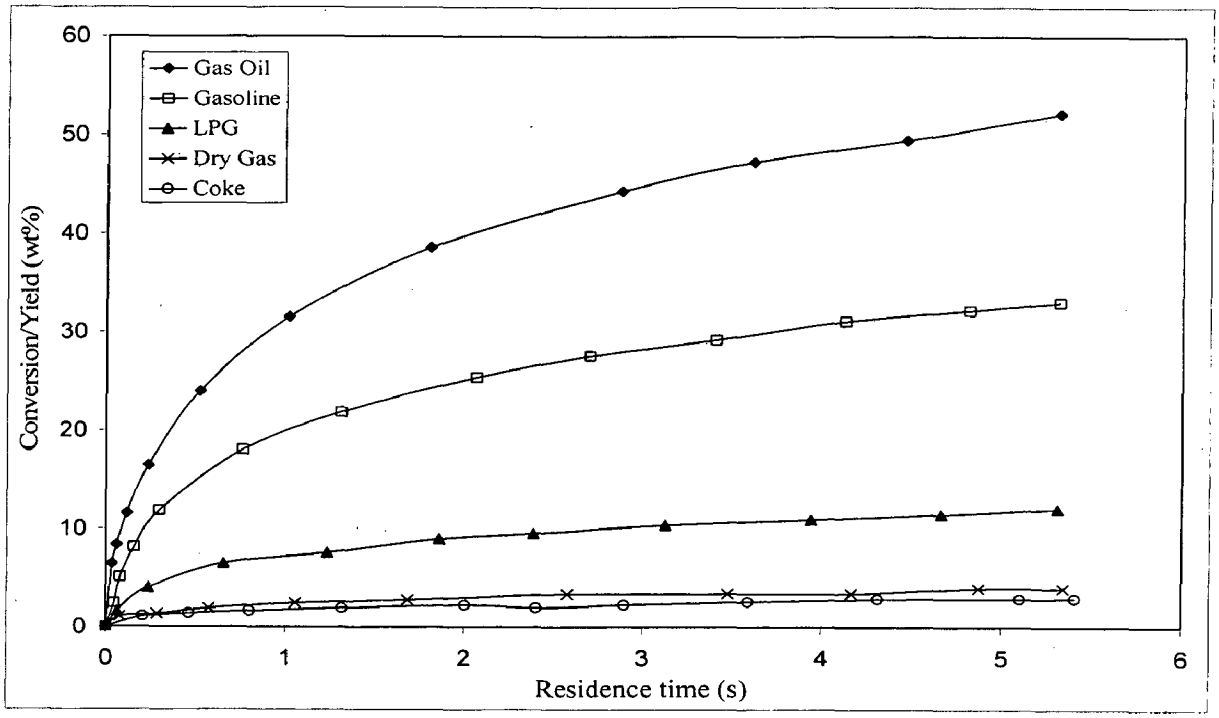

Figure 4.2: Product profile along residence time

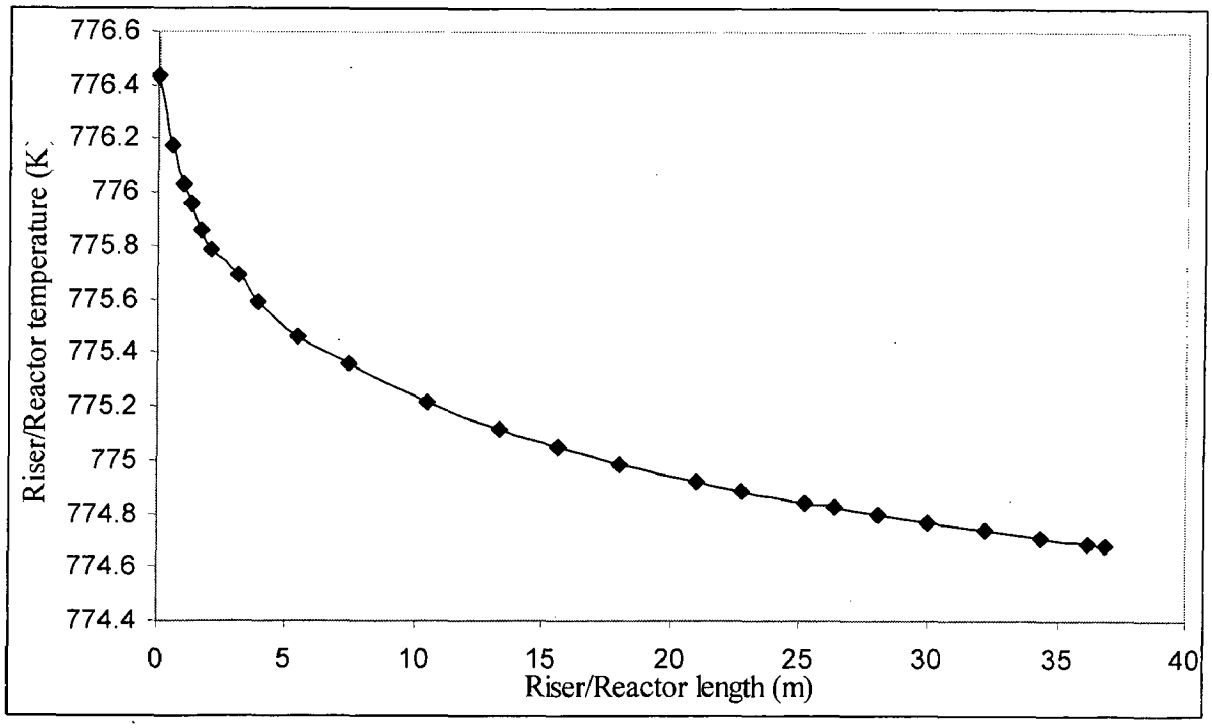

Figure 4.3: Temperature profile along riser length

Figure 4.3: shows that the temperature profile along the riser length while Figure 4.4: shows the same against the residence time in the riser. Since the reactions taking place in the riser are endothermic, a drop in the temperature is expected as one moves up.

The magnitude of the temperature drop obtained is consistent with the industrially observed data as seen from table 4.1.

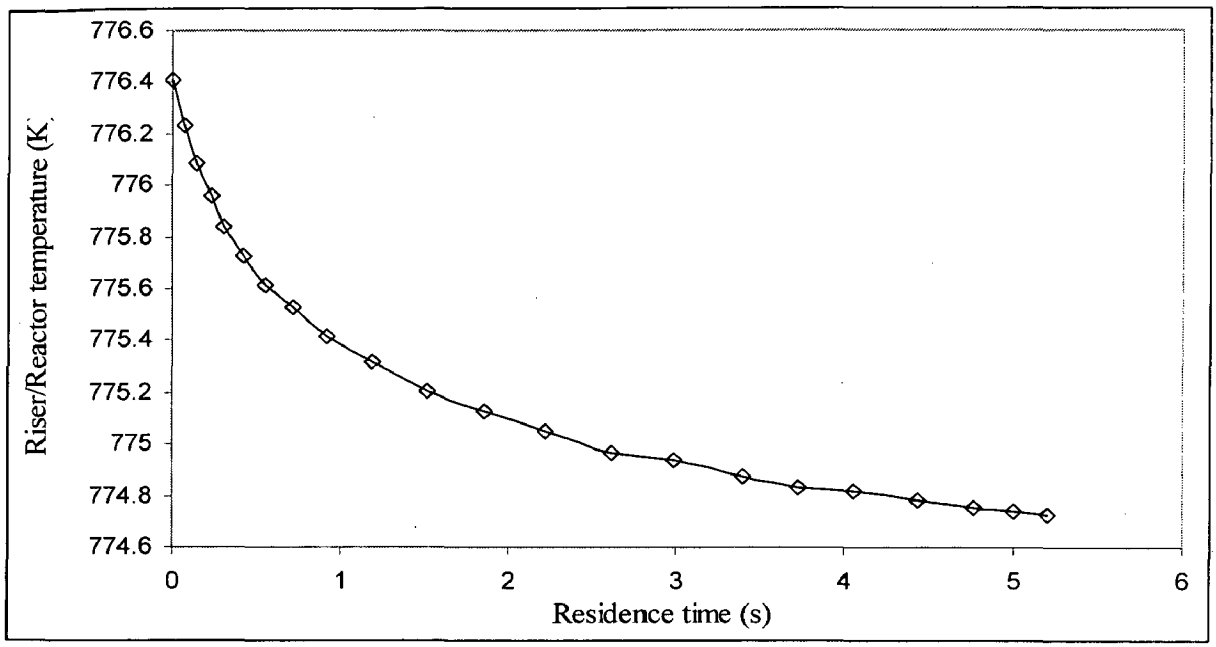

Figure 4.4: Temperature profile against residence time

Figure 4.5 shows that the flow rates of O_2, CO and CO_2 along the regenerated height. As expected oxygen concentrations decrease while due to combustion oxide of carbon are formed.

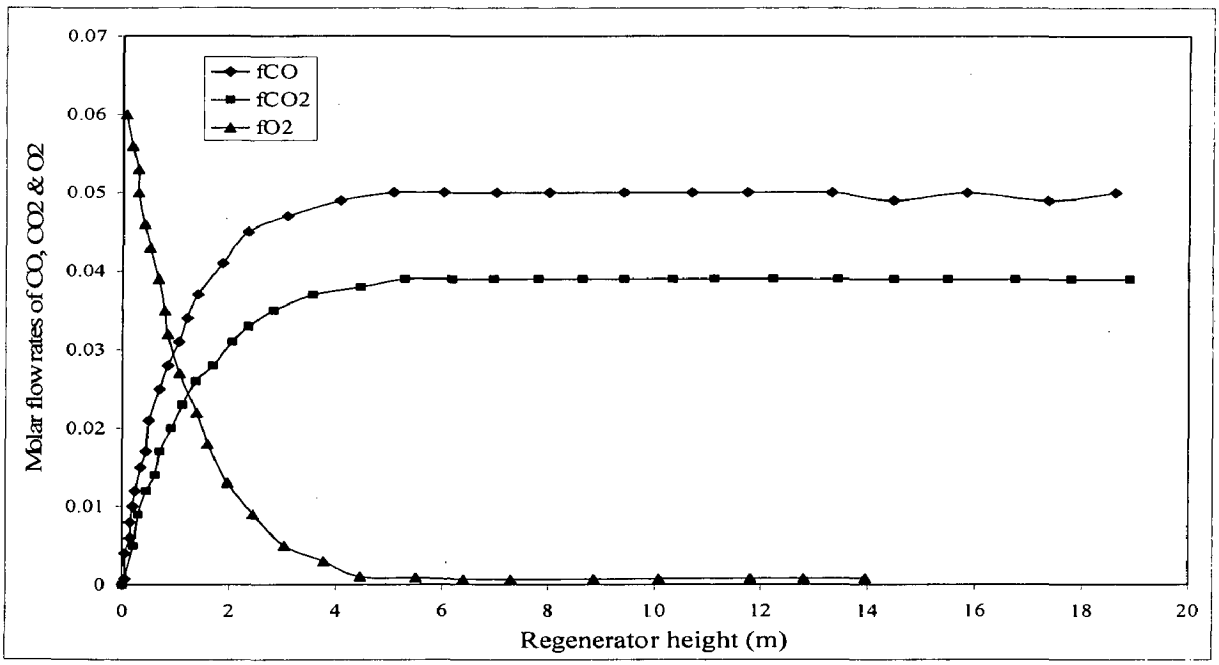

Figure 4.5: Flue gases profile along the regenerator height

4.2 Optimization

The multi-optimization of FCC unit using genetic algorithm and its variants often requires inordinately large amount of computational (CPU) time. The binary-coded elitist non-dominated sorting genetic algorithm (NSGA-II) is adapted, and new code NSGA-II JG, is used to obtain solutions for the multi-objective optimization of FCC unit. This unit is associated with a complex model that is highly compute-intense. The CPU time required for this problem is found to reduce fivefold when NSGA-II JG is used as compared to when NSGA-II is used.

It is observed that the results obtained using NSGA-II using reversion (Figure 3.4 path b), are not very different from those obtained using the original algorithm. However, these results obtained using replacement (Figure 3.4, path a) out performs those obtained by using NSGA-II. Hence NSGA-II JG refers to replacement, i.e., path a of figure 3.4, from now on. Clearly, reversion, a macro-mutation operation, is unable to counteract sufficiently, the genetic uniformly created by elitism, while the macro-mutation operation associated with the replacement is able to do this.

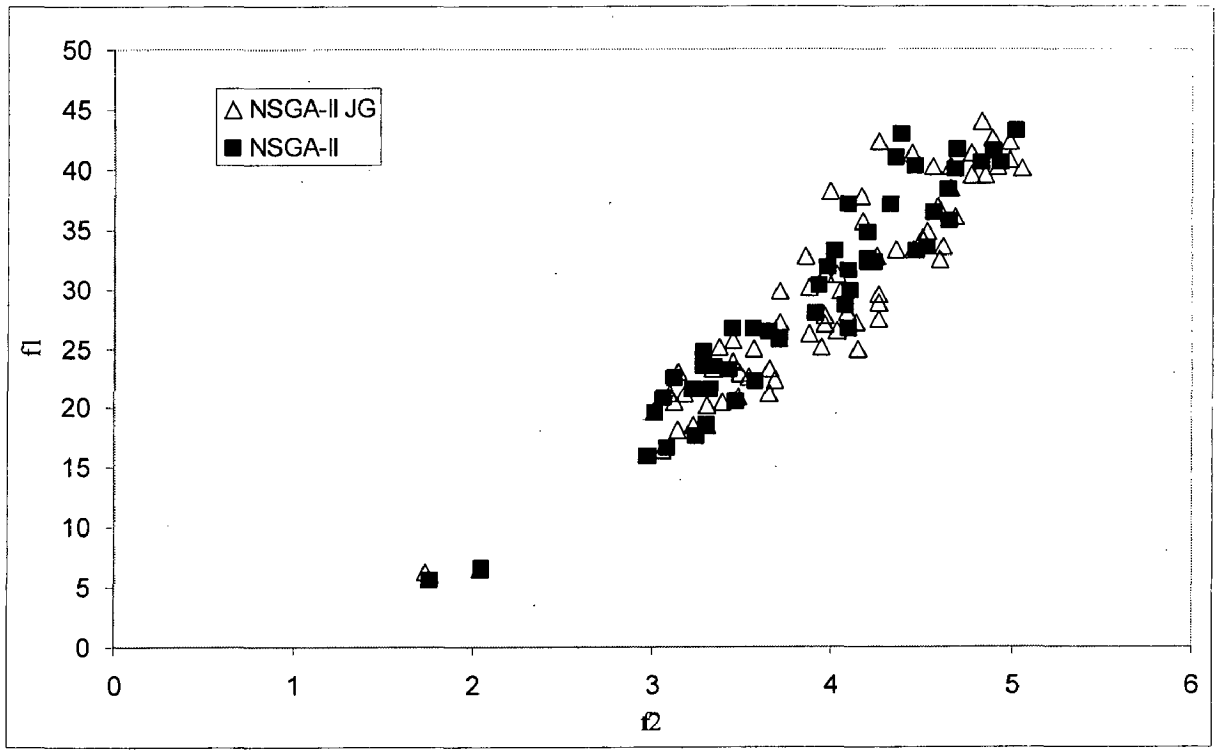

Figure 4.6: For 1 Gen optimization (NSGA-II-JG & NSGA-II)

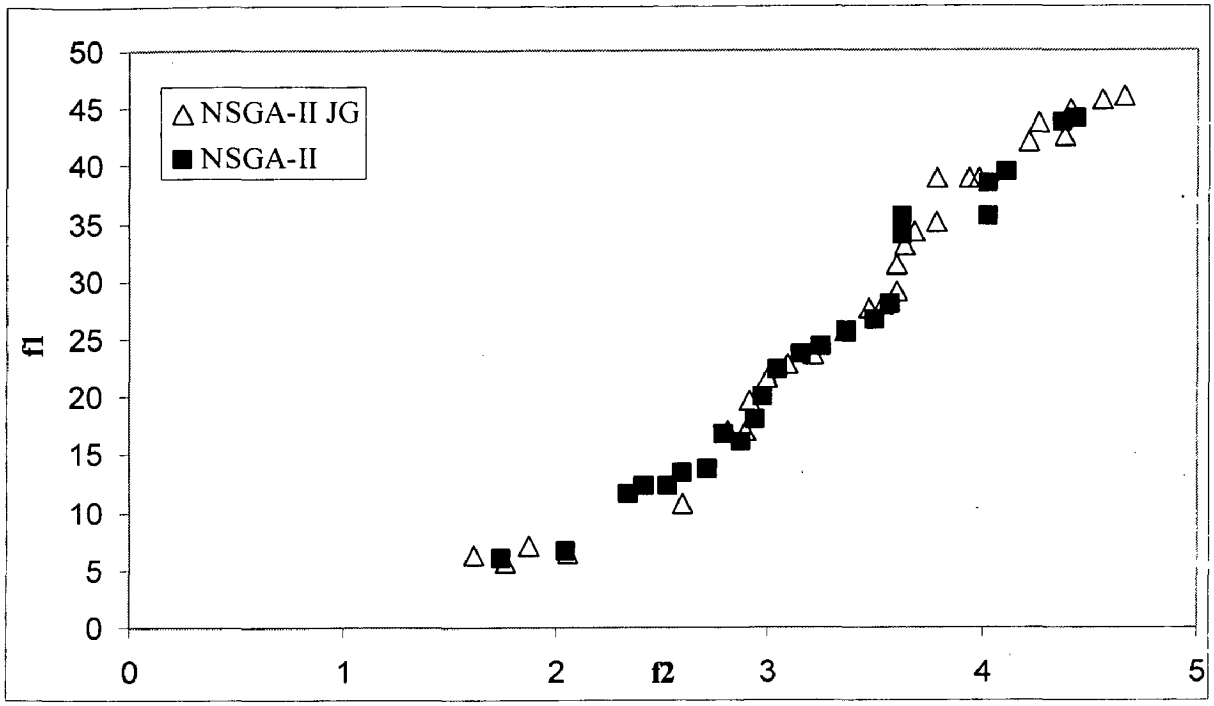

Figure 4.7: For 7 Gen optimization (NSGA-II-JG & NSGA-II)

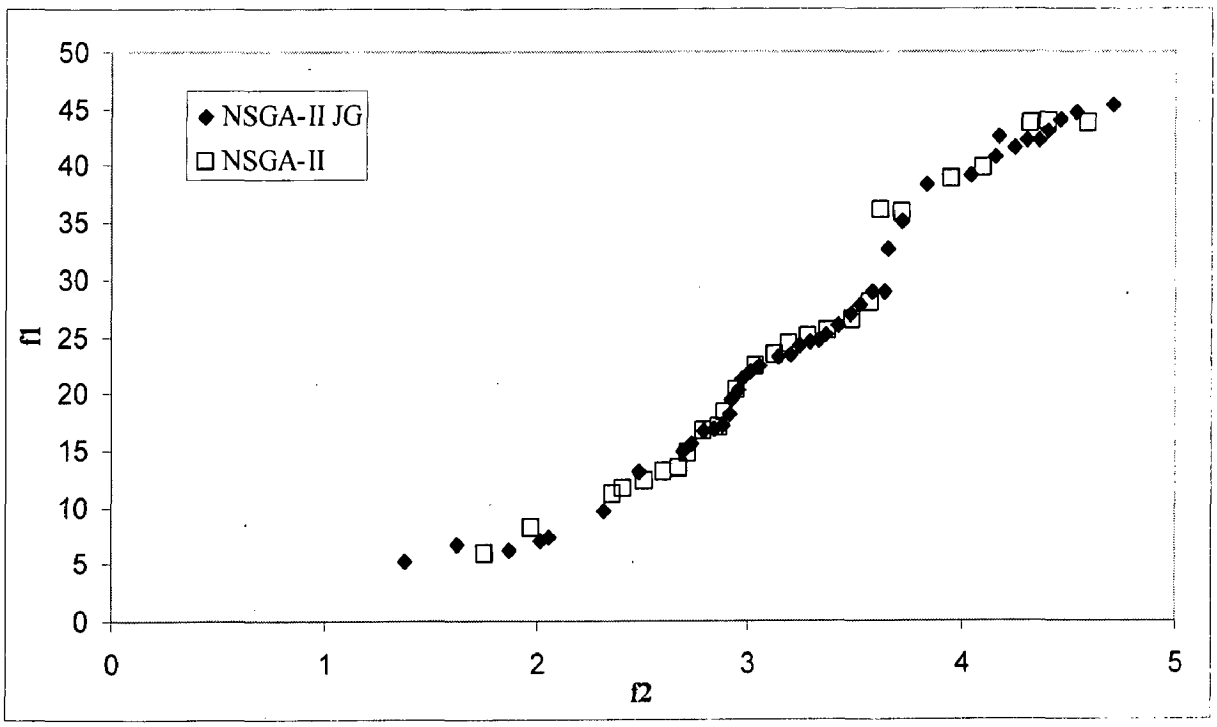

Figure 4.8: For 10 Gen optimization (NSGA-II-JG & NSGA-II)

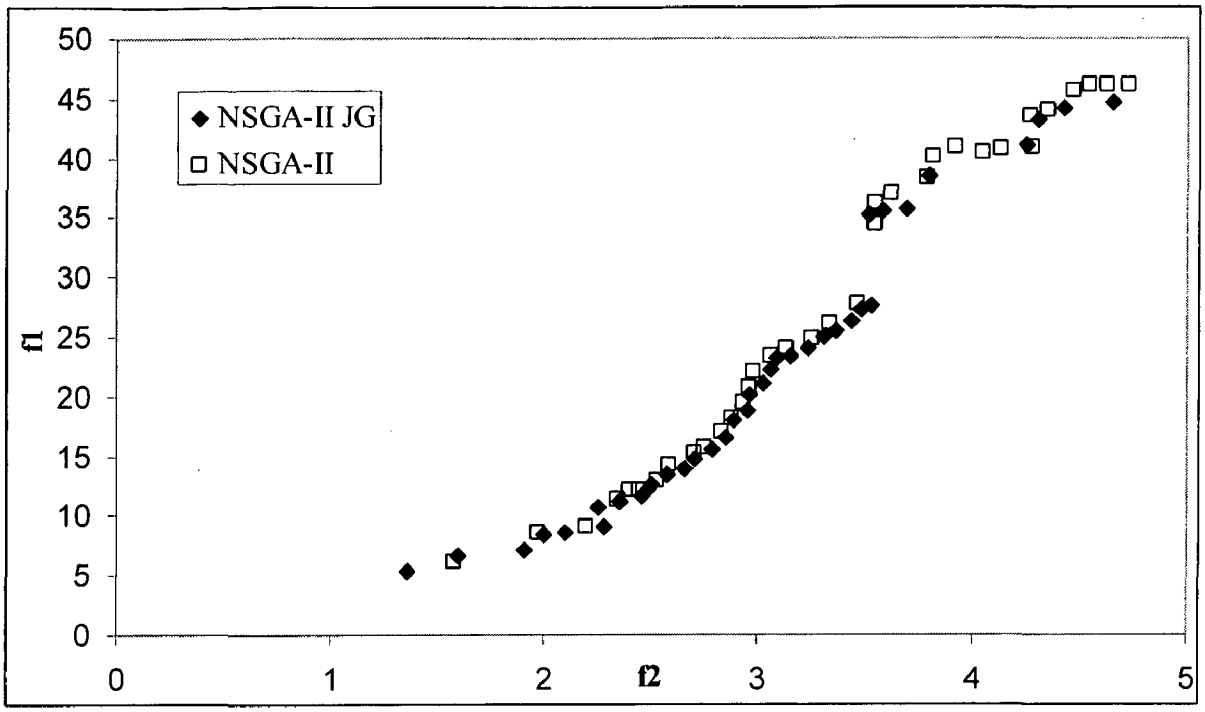

Figure: 4.9: For 50 Gen optimization (NAGA-II-JG & NSGA-II)

Chapter-5

Conclusion& Future Work

CONCLUSIONS & FUTURE WORK

From the present work, it is concluded that the five lump kinetic model predictions are more realistic and closer to the actual results. The advantage of five lumps model that it can predict the coke formation, which supplies the heat required for the heating and vaporization of the feedstock and to perform the endothermic reactions; LPG, which contains important hydrocarbons used together with iso-butane as alkylation and MTBE feeds; and dry gas, which is used as a fuel gas in refinery. But one limitation is that the kinetic model does not consider products heavier than gas oil, such as light cycle oil and heavy cycle oil.

The integrated reactor regenerator model developed in this study is quite simple and makes gross assumptions about hydrodynamics in both the reactor and the regenerator. But the general agreement between predicted and measured yields and other parameters establishes that the assumptions are justified. Such models can be used with advantage in optimizing the operating conditions of FCC units. The type of feed may increase or decrease the gasoline yield, depending upon the composition. A naphthenic feedstock gives maximum yield of gasoline, but at the same time LPG, coke and dry gases yield is also high. Paraffinic feedstock is next, to give the highest yield of gasoline and least yield of coke. Aromatic feedstock gives minimum yield of gasoline.

An empirical model is tuned using some data on an industrial FCC unit. The procedure is quite general and any other FCC unit can be similarly modeled and tuned using associated industrial data. A new method is implemented to optimize the multi-objective function in FCC unit. One can easily infer from the results of the above problem that the binary-coded NSGA-II with the jumping gene adaptation incorporated performs better than the elitist NSGA-II (at least for the problems studied here), both for single as well as multiple objectives. The selected examples extend over a range of complexities, from the simple to a reasonably complex one for an industrial FCC unit. We believe that the increase the diversity through the JG operator compensates for the decrease in diversity associated with elitism. Similar adaptation can be introduced and studied using other multi-objective optimization schemes. Also, this adaptation could

prove quite valuable for solving similar compute-intense multi-objective optimization in chemical engineering.

5.1 Future Work

The some recommendations to follows in future as shown:

1) The five lumps kinetic scheme can be used for more advanced studies of the FCC riser modeling as this scheme facilities the use of more detailed kinetic scheme (for any number pseudocomponenets) for the study of heat and mass transfer effects, adsorption effects, and detailed hydrodynamics.
2) In addition, the effect of feed inlet geometry on the yield of various cracked products is not considered. In future this effect will have to be considered.
3) In future, a three dimensional CFD model, which can predict the effect feed inlet geometry and performance of FCC risers reactors.
4) Unsteady state simulation of riser reactor can also be considered in future.
5) The other optimization can be developed to solve the multi-optimization problem in FCC unit.

References

REFERENCES

1. **Ali, H., and Rohani, S. (1997).** Dynamic modeling and simulation of a riser type fluid catalytic cracking unit. *Chem. Eng. Technol.*, 20, 118-130.
2. **Ali, H., Rohani, S., and Corriou, J.P. (1997).** Modeling and control of a riser type fluid catalytic cracking (FCC) unit. *Transaction of the Institution of Chemical Engineers*, 75, 401-412.
3. **Ancheyta, J.J., Augilar, R.E., and Moreno, M.J. (1997).** A strategy for kinetic parameter estimation in the fluid catalytic cracking process. *Ind. Eng. Chem. Res.*, 36, 5170-5174.
4. **Ancheyta, J.J., Augilar, R.E., and Lopez, I.F., (1999).** 5-lump kinetic model for gas oil catalytic cracking. *Applied Catalysis A: General,* 177, 227-235.
5. **Arbel, A., Hunag, Z., Rinard, I.H., Shinnar, R., and Sapre, A.V. (1995).** Dynamics and control of fluidized catalytic crackers. Modeling of the current generation FCC's. *Ind. Eng. Chem. Res.*, 34, 1228-1243.
6. **Avidan, A.A., and Shinnar, R. (1990).** Development of catalytic cracking technology. A lesson in chemical reactor design. *Ind. Eng. Chem. Res.*, 29, 931-942.
7. **Behie, L.A., and Kehoe, P. (1973).** The grid region in a fluidized bed reactor. *AIChE J.*, 19, 1070-1072.
8. **Berry, T.A., McKeen, T.R., Pugsley, T.S., and Dalai, A.K. (2004).** Two-dimensional reaction engineering model of the riser section of a fluid catalytic cracking unit. *Ind. Eng. Chem. Res.*, 43, 5571-5581.
9. **Bidabehere, C.M., and Sedran, U. (2001).** Simultaneous diffusion, adsorption, and reaction in fluid catalytic cracking catalysts. *Ind. Eng. Chem. Res.*, 40, 530-535.
10. **Blasetti, A., and de Lasa, H, (1997).** FCC riser unit operated in the heat-transfer mode: kinetic modeling. *Ind. Eng. Chem. Res.*, 36, 3223-3229.
11. **Bhaskar, V., Gupta, S.K., and Ray, A.K. (2000).** Application of Multi-objective optimization in Chemical Engineering. *Rev. Chem. Eng.* 16, 1.

12. **Corella, J. (2004).** On the modeling of the kinetics of the selective deactivation of catalysts. Application to the fluid catalytic cracking process. *Ind. Eng. Chem. Res.*, 43, 4080-4086.

13. **Corella, J., Bilbao, R., Molina, J.A., and Artigas, A. (1985).** Variation with time of the mechanism, observable order, and activation energy of the catalyst deactivation by coke in the FCC process. *Ind. Eng. Chem. Process Dev.*, 24, 625-636.

14. **Corella, J., Fernandez, A., and Vidal, J.M., (1986).** Pilot plant for the fluid catalytic cracking unit. Determination of the kinetic parameters of deactivation of the catalyst. *Ind. Eng. Chem. Process Dev.*, 25, 554-562.

15. **Corella, J., and Frances, E. (1991).** Analysis of the riser reactor of a fluid catalytic cracking unit. Model based on kinetics of cracking and deactivation from laboratory tests. In fluid catalytic cracking-II: concepts in catalyst design (edited by Occelli, M.L.) *ACS Symposium Series,* Vol.452, 165-182. Washington: American Chemical Society. (*cf. Gupta and Subba Rao, 2001*).

16. **Corella, J., and Menadez, M. (1986).** The modeling of the kinetics of deactivation of monofunctional catalysts with and acid strength distribution in their non-homogeneous surface. Application of the dectivation of commercial catalysts in the FCC process. *Chem. Eng. Sci.*, 41, 1817-1826.

17. **Coxon, P.G., Bischoff, K.B. (1987).** Lumping strategy, 1. Introduction techniques and application of cluster analysis. *Ind. Eng. Chem. Res.*, 26, 1239-1248.

18. **Das, A.K., Martin, G.B., Heynderickx, G.J. (2003).** Three dimensional simulation of a fluid catalytic cracking riser reactor. *Ind. Eng. Chem. Res.*, 42, 2602-2617.

19. **Dave, D.J., and Saraf, D.N. (2003).** Model for rating and optimization of industrial FCC units. *Indian Chem Engr.*, 45(1), 7-19.

20. **Deb, K. (2001)** Multi-objective optimization using evolutionary algorithms, *Wiley: Chichester, U.K.*

21. **Deb, K., Agrawal, S., and Meryarivan, T. (2000).** A fast Elitist Non-dominated Sorting Genetic Algorithm for multi-objective optimization: NSGA-II.

Proceedings of the Parallel Problem Solving from Nature VI Conference, Paris, September 2000. *Springer: Berlin.*

22. **Davidson, J.F., and Harrison, D. (1963).** Fluidized particle. *London: Cambridge Press.*
23. **de Lasa, H.I., and Grace J.R., (1979).** The influence of the freeboard region in a fluidized bed catalytic cracking regenerator. *AIChE J.*, 25, 984-991.
24. **de Lasa, H.I., Errazu, A., Barreio, E., and Solioz, S. (1981).** Analysis of fluidized bed catalytic cracking regenerator models in a industrial scale unit. *Can. J. Chem. Eng.*, 59, 549-553.
25. **den Hollander, M.A., Makkee, M., and Moulijin, J.A. (2001).** Prediction of the performance of coked and regenerated fluid catalytic cracking catalyst mixtures. Opportunity for process flexibility. *Ind. Eng. Chem. Res.*, 40, 1602-1607.
26. **Derouin, C., Nevicato, D., Forissier, M., Wild, G., and Bernard, J.R. (1997).** Hydrodynamics of riser units and their impact on FCC operation. *Ind. Eng. Chem. Res.*, 36, 4505-4515.
27. **Edward, W.M., and Kimm, H.N. (1988).** Multiple steady states in FCC unit operations. *Chem. Eng. Sci.*, 43, 1825-1830.
28. **Ellis, R.C., Li, Xi., and Riggs, J.B. (1988).** Modeling and optimization of a model IV fluidized catalytic cracking unit. *AIChE J.*, 44, 2068-2079.
29. **Elnashaie, S.S.E.H., and El-Hennawi, I.M (1979).** Multiplicity of steady state in fluidized bed reactors-IV. *Chem. Eng. Sci.*, 34, 1113-1121.
30. **Elnashaie, S.S.E.H., and Elnashini, S.S. (1990).** Digital simulation of industrial fluid catalytic cracking units: Bifurcation and its implementations. *Chem. Eng. Sci.*, 45, 553-559.
31. **Elnashaie, S.S.E.H., Elnashini, S.S., and Alzahrani, S. (1992).** Digital simulation of industrial fluid catalytic cracking units-III. Effect of hydrodynamics. *Chem. Eng. Sci.*, 47, 3152-3156.
32. **Elnashaie, S.S.E.H., Elnashini, S.S. (1993).** Digital simulation of industrial fluid catalytic cracking units-IV. Dynamic behavior. *Chem. Eng. Sci.*, 48, 567-583.
33. **Errazu, A.F., de Lasa, H.I., and Sarti, F. (1979).** A fluidized bed catalytic cracking regenerator model. Grid effects. *Can. J. Chem. Eng.*, 57, 191-197.

34. **Farag, H.. Ng, S., and de Lasa, H. (1993).** Kinetic modeling of catalytic cracking of gas oils using in situ traps (FCCT) to prevent metal contamination. *Ind. Eng. Chem. Res.*, 32, 1071-1080.

35. **Flinger, M. Schipper, P.H., Sapre, A.V., and Krambeck, F.J., (1994).** Two phase cluster model in riser reactors: Impact of radial density distribution on yields. *Chem. Eng. Sci.*, 49, 5813-5818.

36. **Fogler, H.S. (1992).** Elements of chemical reaction engineering (2^{nd} edition, pp.62). *New Delhi: Prentice-Hall of India.*

37. **Gao J., Xu, C., Lin, S., Yang, G., and Guo, Y. (1999).** Advanced model for turbulent gas solid and reaction in FCC riser reactors. *AIChE J.*, 45, 1095-1113.

38. **Gao J., Xu, C., Lin, S., Yang, G., and Guo, Y. (2001).** Simulation of gas-liquid-solid 3-phase and reaction in FCC riser reactors. *AIChE J.*, 47, 677-692.

39. **Geldart, D. (1973).** Types of gas fluidization. Powder Technology, 7, 677- 681.

40. **Gianetto, A., Faraq, H., Blasetti, A., and de Lasa, H. (1994).** FCC catalyst for reformulated gasolines. Kinetics modeling. *Ind. Eng. Chem. Res.*, 33, 3053-3062.

41. **Gidaspow, D., and Hulin, L. (1998).** Equation of state and radial distribution functions of FCC particles in a CFB. AIChE. J., 44, 279-293.

42. **Godfroy, L., Patience,G.S., and Chauki, J. (1999).** Radial hydrodynamics in risers. *Ind. Eng. Chem. Res.*, 38, 81-89.

43. **Gross, B., Jacob, S.M., Nace, D.M., and Voltz, S.E. (1976).** Simulation of catalytic cracking process. US Patent 3960707. *(cf. Arbel et al., 1995)*

44. **Gross, B., Nace, D.M., and Voltz, S.E. (1974).** Application of a kinetic model for comparison of catalytic cracking in fixed bed microreactor and a fluidized dense bed. *Ind. Eng. Chem. Process Des. Dev.*, 13, 199-203.

45. **Gupta, A., and Subba Rao, D. (2001).** Model for the performance of a fluid catalytic cracking (FCC) riser reactor: Effect of feed atomization. *Chem. Eng. Sci.*, 56, 4489-4503.

46. **Gupta, A., and Subba Rao, D. (2003).** Effect of feed atomization on FCC performance: simulation of entire unit. *Chem. Eng. Sci.*, 58, 4567-4579.

47. **Han, I.S., Chung, C.B., and Riggs, J.B. (2000).** Modeling of fluidized catalytic cracking process. *Comput. Chem. Eng.*, 24, 1681-1687.

48. **Iscol, L. (1970).** The dynamics and stability of a fluid catalytic cracker. In proceedings of *joint Automatic Control Conference*, Atlanta, Georgia, 602-607. (*cf. Ali and Rohani, 1997*).

49. **Jacob, S.M., Gross, B., Voltz, S.E., and Weekman, V.W., Jr. (1976).** A lumping and reaction scheme for catalytic cracking. *AIChE. J.*, 22, 701-713.

50. **Kasat, R.B., Kunzuru, D., Saraf, D.N., and Gupta, S.K. (2002).** Multi-optimization of industrial FCC units using Elitist Non-dominated Sorting Genetic Algorithm. *Ind. Eng. Chem. Res.*, 41, 4765-4776.

51. **Khandalekar, P.D., and Riggs, J.B. (1995).** Nonlinear process model based control and optimization of model IV FCC unit. *Comput. Chem. Eng.*, 19, 1153-1168.

52. **Kimm, N.K., Berruti, F., and Pugsley, T.S. (1996).** Modeling the hydrodynamics of down flow gas solid reactors. *Chem. Eng. Sci.*, 51, 2661-2666.

53. **Kraemer, D., Larocca, M., and de Lasa, H.I. (1991).** Deactivation of cracking catalyst in short contact time reactors: Alternative models. *Can. J. Chem. Eng.*, 69, 355-360.

54. **Krishna, A.S., and Parkin, E.S. (1985).** Modeling the regenerator in commercial fluid catalytic cracking units. *Chem. Eng. Prog.*, 31 (4), 57-62.

55. **Kumar, S., Chadha, A., Gupta, R., and Sharma, R., (1995).** CATCRACK: A process simulator for an integrated FCC regenerator system. *Ind. Eng. Chem. Res.*, 34, 3737-3748.

56. **Kunni, D., and Lavenspiel, O. (1969).** Fluidization Engineering, *Wiley, New York.*

57. **Larocca, M., Ng, S., and de Lasa, H. (1990).** Catalytic cracking of heavy gas oils: Modeling coke deactivation. *Ind. Eng. Chem. Res.*, 29 (2), 171-180.

58. **Lee, L., Chen, Y., Huang, T. and Pan, W. (1989a).** Four lump kinetic model for fluid catalytic cracking process. *Can. J. Chem. Eng. J.*, 67, 615-619.

59. **Lee, L., Yu, S., Cheng, C., and Pan, W. (1989b).** Fluidized bed catalytic cracking regenerator modeling and analysis. *Chem. Eng. J.*, 40, 71-82.

60. **Martin, M.P., Derouin, P.T., Forissier, M., Wild, G., and Bernard, J.R. (1992).** Catalytic cracking in riser reactors. Core-annulus and elbow effects. *Chem. Eng. Sci.*, 47, 2319-2324.

61. **Maxwell, J.B. (1968).** Data book on hydrocarbons. *New York: Robert E. Krieger Publishing Co., Inc.*

62. **Mirgain C., Briens, C., Pozo, M.D. Loutaty, R., and Bergougnou, M. (2000).** Modeling feed vaporization in fluid catalytic. *Ind. Eng. Chem. Res.*, 39, 4392-4399.

63. **Morley, K., and de Lasa, H. (1987).** On the determination of kinetic parameters for the regeneration of cracking catalyst. *Can. J. Chem. Eng.*, 65, 773-783.

64. **Murphy, J.R. (1992).** Evolutionary design changes mark FCC process. *Oil Gas J.*, 90 (20), 49-58.

65. **Nace, D.M. (1970).** Catalytic cracking over crystalline alumino-silicates. Micro-reactor study of gas oil cracking. *Ind. Eng. Chem. Process Des. Dev.*, 9(2), 203-209.

66. **Nace, D.M. Voltz, S.E., and Weekman, V.W., Jr. (1971).** Application of a kinetic model for catalytic cracking. Effects of charge stocks. *Ind. Eng. Chem. Process Des. Dev.*, 10, 530-537.

67. **Pareek, V.K., Adesina, A.A., Srivastava, A., and Sharma, R. (2002).** Senstivity analysis of rate constants of Weekman;s riser kinetics and evolution of heat of cracking using CATCRACK. *Journal of Molecular catalysis A,* 181, 263-274.

68. **Pareek, V.K., Adesina, A.A., Srivastava, A., and Sharma, R. (2003).** Modeling of a non-isothermal FCC riser. *Chem. Eng. J.*, 92, 101-109.

69. **Pitault, I., Nevicato, D., Forissier, M., and Bernard, J.R. (1994).** Kinetic model on a molecular description for catalytic cracking of vacuum gas oil. *Chem. Eng. Sci.*, 49, 4249-4262.

70. **Pugsley, T.S., Berruti, F.A. (1996).** Predictive hydrodynamics model for circulating fluidized bed risers. *Powder Technology,* 89, 57-69.

71. **Samuelsberg, A., and Hjertager, B.H. (1996).** Computational modeling of gas/particle flow in a riser. *AIChE J.*, 42, 1536-1546.

72. **Shah, Y.T., Huling, G.T., Paraskos, J.A., and Mckinney, J.D. (1977).** A kinematic model for an adiabatic transfer line catalytic cracking reactor. *Ind. Eng. Chem. Process Des. Dev.*, 16(1), 89-94.

73. **Sundaresan, S. (2000).** Modeling the hydrodynamics of multiphase flow reactors: Current status and challenges. *AIChE .J.*, 46, 1102-1105.

74. **Takatsuka, T., Sato, S. Morimato, Y., and Hashimato, H. (1987).** A reaction model for fluidized-bed catalytic cracking of residual oil. *Int. Chem. Eng.*, 27 (1), 107-116.

75. **Theologos, K.N., Lygeros, A.I., Markatos, N.C. (1999).** Feedstock atomization effects on FCC riser reactors selectivity. *Chem. Eng. Sci.*, 54, 5369-5376.

76. **Theologos, K.N., and Markatos, N.C. (1993).** Advanced modeling of fluid catalytic cracking riser-type reactors. *AIChE. J.*, 39, 1007-1017.

77. **Theologos, K.N., Nikou, I.D., Lygeros, A.I., and Markatos, N.C. (1997).** Simulation and design of fluid catalytic cracking riser type reactors. *AIChE. J.*, 43, 486-493.

78. **Wang, L., Yang, B., and Wang, Z. (2005).** Lumps and kinetics for the secondary reactions in catalytically cracked gasoline. *Chem. Eng. J.*, 109, 1-9.

79. **Weekman, V.W., Jr. (1968).** A model of catalytic cracking conversion in fixed, moving, and fluid-bed reactors. *Ind. Eng. Chem. Process Des. Dev.*, 7, 90-95.

80. **Weekman, V.W., Jr. (1969).** Lumps models and kinetics in practice. *AIChE Monograph Series 11*, 75, 3-29.

81. **Wilson, J.W. (1997).** Fluid catalytic cracking technology and operations. *Oklahoma: Penn Well Publishing Company.*

82. **Yen, L.C., Wrench, R.E., and Kuto, C.M. (1985).** FCCU Regenerator temperature effects evaluated. *Oil Gas J.*, 83, 67-70.

83. **Zheng,** Y.**Y.(1994).** Dynamic modeling and simulation of a catalytic cracking unit. *Comput. Chem. Eng.*, 18, 39-44.

84. **Zhou, J., Grace, J.R., Qin, S., Brereton, C.M.H., Lim, C.J., and Zhu, J., (1994).** Voidage profiles in a circulating fluidized bed of square cross-section. *Chem. Eng. Sci.*, 49, 3217-3226.

Nomenclature

NOMENCLATURE

A = cross-sectional area of regenerator, ft^2

A_{rgn} = cross-sectional area of regenerator, m^2

A_{ris} = cross-sectional area of riser, m^2

C_c = coke on catalyst at any location, (kg of coke) (kg of catalyst)$^{-1}$

C_i = concentration of ith lump, kmol m^{-3}

C_H = weight fraction of H_2 in coke, (kg of H_2) (kg of coke)$^{-1}$

C_{rgc} = coke on regenerated catalyst, (kg of coke) (kg of cat)$^{-1}$

C_{sc} = coke on spent catalyst, (kg of coke) (kg of cat)$^{-1}$

C_{pc} = heat capacity of catalyst, kJ kg^{-1} K^{-1}

C_{pfl} = heat capacity of liquid feed, kJ kg^{-1} K^{-1}

C_{pfv} = heat capacity of vapor feed, kJ kg^{-1} K^{-1}

C_{pi} = mean heat capacity of i [H_2O, N_2, O_2], kJ kg^{-1} K^{-1}

C_{ptot} = heat capacity of (total) mixture, kJ kg^{-1} K^{-1}

D = diameter of regenerator, ft

D_p = average diameter of catalyst particle, ft

E_c, E_β = activation energies, kJ kmol^{-1}

E_i = activation energy of ith reaction, kJ kmol^{-1}

f_i = molar flow rate of i [CO, CO_2, H_2O, N_2, O2, carbon] in the regenerator, kmol s^{-1}

f_{tot} = total gas flow rate at any location in the regenerator, kmol s^{-1}

F_{air} = flow rate of air feed to the regenerator, kmol s^{-1}

F_{ent} = entrained catalyst flow rate, kg s^{-1}

F_{feed} = feed flow rate of oil, kg s^{-1}

F_j = molar flow rate of jth lump, kmol s^{-1}

F_{rgc} = flow rate of regenerated catalyst, kg s^{-1}

F_{sc} = flow rate of spent catalyst, kg s^{-1}

g = gravitational acceleration, 32.2 ft s^{-2}

h = dimensionless height of riser ($\equiv z/H_{ris}$)

ΔH_{evp} = heat of vaporization of gas oil feed, kJ kg^{-1}

H_i = heat of formation of i, kJ kmol^{-1}

ΔH_i = heat of ith reaction, kJ $kmol^{-1}$

H_{ris} = height of riser, m

$k_{0,i}$ = frequency factor for ith reaction

k_c = overall rate of combustion of coke

k_i = reaction rate constant for ith reaction

MW_c = molecular weight of coke, kg $kmol^{-1}$

MW_g = average molecular weight of gas phase, kg $kmol^{-1}$

MW_j = molecular weight of jth lump, j = 1, 2, ..., 5, kg $kmol^{-1}$

MW_H = molecular weight of H_2, kg kmol-1

N_{chr} = total chromosome length (40)

N_{ga} = number of generations (50)

N_p = population size (50)

p_c = crossover probability (0.95)

p_m = mutation probability (0.05)

P_{rgn} = pressure in regenerator, atm

P_{ris} = pressure in riser, atm

r_i = rate of the ith reaction, i = 1-9 (riser); i = 10-12 (regenerator), kmol (kg catalyst)$^{-1}$ s^{-1} or kmol $m^{-3}s^{-1}$

R = universal gas constant, J K^{-1} $kmol^{-1}$

T_{air} = temperature of air fed to the regenerator, K

T_{base} = base temperature for heat balance calculations, K (assumed, 866.6 K)

T_{dil} = temperature of dilute phase at any location, K

T_{feed} = temperature of gas oil feed, K

T_{rgn} = temperature (uniform) of dense bed, K

T_{ris} = temperature of riser at any location, K

$T_{ris,\,top}$ = temperature at top of riser, K

T_{sc} = temperature of spent catalyst [= $T_{ris,\,top}$ - ΔT_{st}], K

ΔT_{st} = temperature drop in stripper (assumed 10 K)

u = velocity of gas in the riser or the regenerator, m s^{-1}

u_l = superficial linear velocity, ft s^{-1}

W = catalyst entrainment flux, lb (ft^2 regenerator area)$^{-1}$ s^{-1}

x_j = mole fraction of jth lump, j = 1, 2, ..., 5

x_{pt} = relative (catalytic) CO combustion rate

Y = (kg catalyst entrained in dilute phase) (kg fluidizing vapor)$^{-1}$

z = height from the entrance of the regenerator, m

Z_{bed} = height of the dense bed, m

Z_{dil} = height of the dilute phase, m

Z_{rgn} = total height of the regenerator, m

Greek Letters

α_{ij} = stoichiometric coefficient of jth species in ith reaction, based on mass

β_c = CO/CO_2 ratio at catalyst surface in regenerator

ε = void fraction in riser or regenerator at any location

ε_{dil} = void fraction in the dilute phase at any location

ρ_c = density of solid catalyst (not including void fraction), kg m^{-3}

ρ_{den} = density of catalyst in the dense bed, kg m^{-3}

ρ_{dil} = density of catalyst in the dilute phase, kg m^{-3}

ρ_f = density of fluidization vapor, lb ft^{-3}

ρ_g = density of gas phase in the regenerator, kmol m^{-3}

ρ_p = density of catalyst particle (solid), lb ft^{-3}

ρ_v = density of vapor at any location, kg m^{-3}

φ =activity of the catalyst

Subscripts

i, j = ith or jth lump (1, gas oil; 2, gasoline; 3, LPG; 4, dry gas; 5, coke)

Appendix-I

Selection of Feed Characterization & Properties of Pseudocomponents

SELECTION OF FEED CHARACTERIZATION & PROPERTIES OF PSEUDOCOMPONENTS

Petroleum fractions are mixtures of innumerable components which are difficult to be identified individually. However, Watson characterization factor can be treated as an approximate indicator of the various groups of compounds (such as paraffin, olefin, naphthene, aromatic, etc) present in the petroleum fraction. Watson and Nelson (1933) made remarkable observation that the factor K_W ($=T_b^{1/3}/sg$), known as Watson characterization factor, is closer to 12 for paraffins and olefins, approximately 10 for aromatics and the 11 and 12 for naphthenes when the normal boiling point of the component Tb is in Rankin and sg is the specific gravity at 60°/60°F .

The characterization factor of the mixture of hydrocarbons is given by $K_W=MeABP^{1/3}/sg$, where, MeABP is the mean average boiling point of the mixture (**API data book, Chapter 2, Characterization of hydrocarbons, 1976**). Using this, **Miquel and Castells, (1993)** proposed a method along with a computer program (**Miquel and Castells, 1994**) that can represent an oil fraction by a mixture of small number of hypothetical components or pseudocomponents. To use this approach atmosphere true boiling point (TBP) distillation curve and the entire fraction density is required. this method assumes that if the difference in final boiling point (FBP) and initial boiling point (IBP) of a petroleum fraction is not too high (i.e., <300 K) then the Watson characterization factor of any narrow-boiling fraction of this mixture (boiling range between 15 to 25 K) remains equal to that of original fraction.

In the present case, due to unavailability of TBP curve for the FCC feed, simulated distillation (SD) curve reported by **Pekediz et al. (1997)** was used. The SD curve was first converted to ASTM-D86 curve and then to TBP data is given in TableA1-1. To generate pseudocomponents, the TBP curve of the feed was divided into twelve parts, out of which four were of 5 volume% each and eight of 10 volume% each (shown as vertical bars in figure A1.1).These vertical bars represent twelve pseudocomponent of the feed. The boiling point of each individual pseudocomponent was determined by area-averaging of the TBP curve (clearly visible in figure A1.1). Considering constant Watson

characterization factor, specific gravity of each pseudocomponent was determined by the equation.

$$sg = 1.21644 \frac{T_b^{1/3}}{K_W}$$

Where, T_b is in K

Table A1.1: Distillation data of hydrocarbon feed (Perkediz et al., 1997)

Volume % Distilled	SD (K)	ASTM-D86* (K)	TBP* (K)
IBP	532	585.5	558.9
10 wt %	587	615.5	604.3
30 wt %	621	632.8	636.4
50 wt %	650	652.3	665.3
70 wt %	683	680.5	665.3
90 wt %	730	721.4	743.9
FBP	800	756.6	808.1

Density of feed (at 15°C) = 929.20 kg/m^3

*Estimated using correlation proposed by **Daubert (1994)**

Molecular weight of these pseudocomponents were then calculated by the following equation proposed by **Edmister and Lee (1984)** which requires knowledge of boiling point and the specific gravity of a hydrocarbon fraction.

$$MW = 204.38\, e^{(0.00218\, T_b)}\, e^{(-3.07\, sg)}\, T_b^{0.118}\, sg^{1.88}$$

Having known values of the volume fraction, boiling point, specific gravity, and molecular weight, each individual bars of Figure A1.1 can be treated as a pure component (of course, hypothetical pure component or pseudocomponent). To make use of the above equations, an iterative method has to be adopted as the value of Watson characterization factor is not known beforehand. **Miquel and Castells (1993 & 1994)** have explained this iterative approach in detail.

After breaking the FCC unit feed into pseudocomponents, and determining the exact value of Watson characterization factor, properties of other 31pseudocomnents were also determined by using above equation. Boiling points of these 31

pseudocomponents were taken at equal interval between the boiling point of n-pentane and the boiling of first pseudocomponent of FCC unit feed (570 K in the present case). The lightest seven components were taken as pure paraffin which is the major constituent of gases. Initially, volume fraction of all these seven pure components and 31 pseudocomponents, which are not present in feed, were taken zero. Thus total fifty components (seven pure components and forty three pseudocomponents) were considered in the present approach for the simulation of FCC riser reactor.

After determining normal boiling point, specific gravity, and molecular weight of all pseudocomponents, heat capacities were determined using the correlations of **Kesler and Lee (1976)** and heat of combustion by equation (Table A1.2).

Predicted concentrations of pseudocomponents in the product stream are given in Figure A1.2. Also, various product streams, viz., gas, gasoline, LCO, and residue are marked on the basis of boiling points.

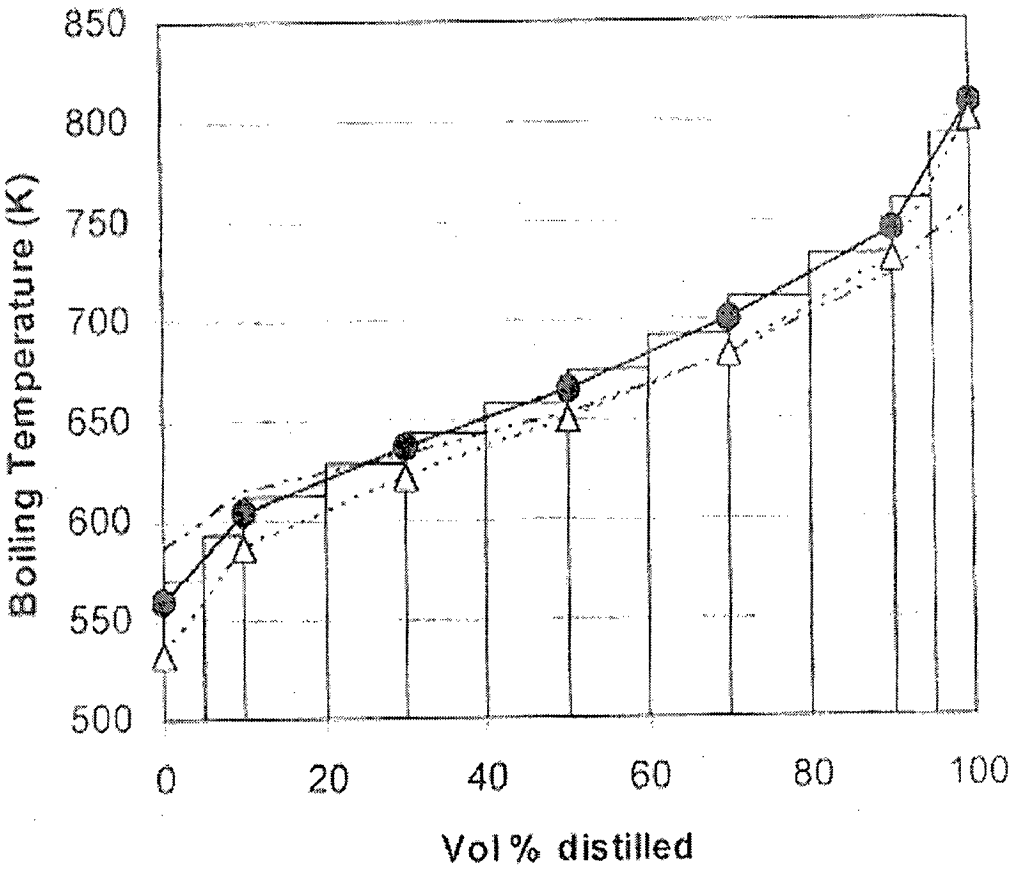

Figure A1-1: Pseudocomponents generated from feed TBP

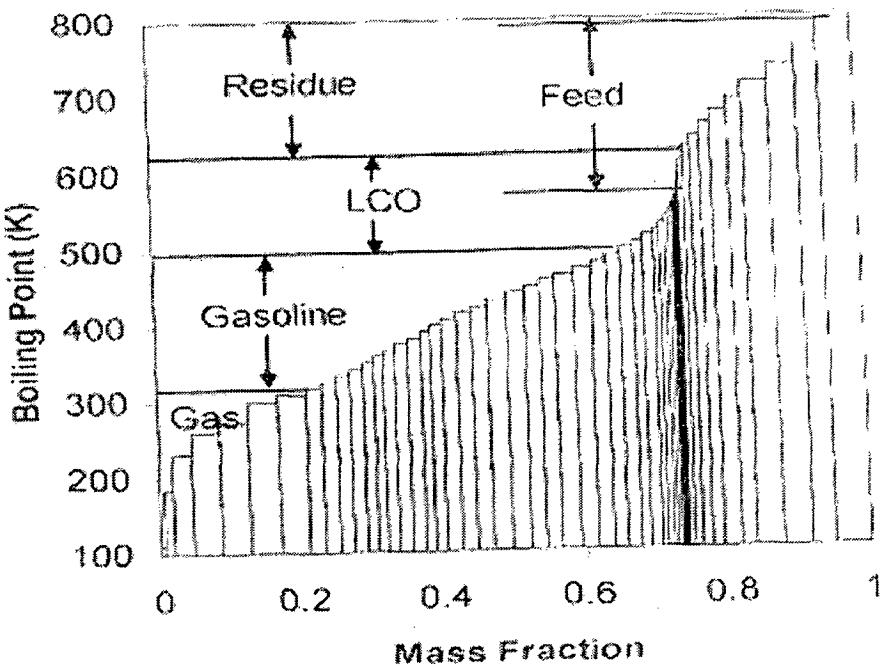

Figure A1-2: Mass fraction of pseudocomponents in the product

TableA1.2 Properties of pseudocomponents (PC_1 to PC_7 are pure components; PC_8 to PC_{29} constitute gasoline fraction; PC_{30} to PC_{41} constitute light cycle oil fraction; PC_{42} to PC_{50} to constitute residual fraction whereas feed contains PC_{39} to PC_{50})

Component	Component name	Boiling Point (K)	Molecular weight	$\Delta H_{comb\ (kJ/kmol)^*}$
PC_1	Methane	111.65	16.043	62764.79
PC_2	Ethane	184.50	30.070	58622.94
PC_3	Propane	231.09	44.097	51983.86
PC_4	i-Butane	261.43	58.124	50464.83
PC_5	n-Butane	272.65	58.124	49960.31
PC_6	i-Pentane	300.98	72.150	49073.02
PC_7	n-Pentane	309.21	72.150	48952.84
PC_8	Pseudocomponent	317.37	88.563	47318.37
PC_9	Pseudocomponent	325.54	91.443	47226.62
PC_{10}	Pseudocomponent	333.70	94.402	47137.89
PC_{11}	Pseudocomponent	341.86	97.443	47052.01

PC_{12}	Pseudocomponent	350.03	100.569	46968.81
PC_{13}	Pseudocomponent	358.19	103.781	46888.17
PC_{14}	Pseudocomponent	366.35	107.083	46809.94
PC_{15}	Pseudocomponent	374.52	110.478	46734.00
PC_{16}	Pseudocomponent	382.68	113.969	46660.24
PC_{17}	Pseudocomponent	390.84	117.558	46588.54
PC_{18}	Pseudocomponent	399.01	121.249	46517.73
PC_{19}	Pseudocomponent	407.17	125.045	46445.89
PC_{20}	Pseudocomponent	415.33	128.948	46373.59
PC_{21}	Pseudocomponent	423.50	132.964	46300.89
PC_{22}	Pseudocomponent	431.66	137.094	46227.80
PC_{23}	Pseudocomponent	439.83	141.343	46154.34
PC_{24}	Pseudocomponent	447.99	145.713	46080.57
PC_{25}	Pseudocomponent	456.15	150.210	46006.47
PC_{26}	Pseudocomponent	464.32	154.835	45032.07
PC_{27}	Pseudocomponent	472.48	159.595	45857.39
PC_{28}	Pseudocomponent	480.64	164.491	45782.42
PC_{29}	Pseudocomponent	488.81	169.530	45707.18
PC_{30}	Pseudocomponent	496.97	174.714	45631.67
PC_{31}	Pseudocomponent	505.13	180.049	45555.89
PC_{32}	Pseudocomponent	513.30	185.538	45479.85
PC_{33}	Pseudocomponent	521.46	191.187	45403.53
PC_{34}	Pseudocomponent	529.62	197.000	45326.93
PC_{35}	Pseudocomponent	537.79	202.982	45250.05
PC_{36}	Pseudocomponent	545.95	209.138	45172.88
PC_{37}	Pseudocomponent	554.11	215.474	45095.39
PC_{38}	Pseudocomponent	562.28	221.995	45017.59
PC_{39}	Pseudocomponent	570.44	228.706	44939.46
PC_{40}	Pseudocomponent	593.12	248.399	44730.49
PC_{41}	Pseudocomponent	612.48	266.496	44531.20

PC_{42}	Pseudocomponent	628.50	282.446	44353.16
PC_{43}	Pseudocomponent	643.76	298.497	44187.51
PC_{44}	Pseudocomponent	658.25	314.656	44034.96
PC_{45}	Pseudocomponent	674.30	333.352	43871.15
PC_{46}	Pseudocomponent	691.91	355.231	43697.31
PC_{47}	Pseudocomponent	711.55	381.318	43510.14
PC_{48}	Pseudocomponent	733.25	412.311	43311.36
PC_{49}	Pseudocomponent	760.13	454.185	43075.64
PC_{50}	Pseudocomponent	792.20	509.673	42808.56

Appendix-II

Elitist Non-dominated Sorting Genetic Algorithm with Jumping Gene, NSGA-II JG

ELITIST NON-DOMINATED SORTING GENETIC ALGORITHM WITH JUMPING GENE, NSGA-II JG

Note: The following assumes that we are minimizing all the objective functions, f_q

(1) Generate box, P, of N_p parent chromosomes using a random-number code to generate the several binaries. These chromosomes are given a sequence (position) number as generated

(2) Classify these chromosomes into fronts based on non-domination (**Deb, 2001**), as follows:

a) Create new (empty) box, P', of size, Np

b) Transfer ith chromosome from P to P', starting with i=1

c) Compare chromosome i with each member, say, j, already present in P', one at a time

d) If i dominates (**Deb, 2001**) over j (i.e. i is superior to or better than j in terms of all objective functions), remove the jth chromosome from P' and it put it back in its original location in P

e) If i is dominated over by j, remove i from P' and put it back in its position in P

f) If i and j are non-dominating (i.e. there is at least one objective function associated with i that is superior to/better than that of j), keep both i and j in P' (in sequence). Test for all j present in P'

g) Repeat for next chromosome (in the sequence, without going back) in P till all N_p are tested. P' now contains a sub-box (of size5 N_p) of non-dominated chromosomes (a subset of P), referred to as the first front or sub-box. Assign it a rank number, I_{rank}, of 1

h) Create subsequent fronts in (lower) sub-boxes of P', using Step 2b above (with the chromosomes remaining in P). Compare these members only with members present in the current sub-box, and not with those in earlier (better) sub-boxes. Assign these I_{rank}=2, 3,. . . Finally, we have all N_p chromosomes in P', boxed into one or more fronts

(3) Spreading out: Evaluate the crowding distance, $I_{i,dist,}$ for the ith chromosome in any front, j, of P' using the following procedure:

a) Rearrange all chromosomes in front j in ascending order of the values of any one (say, the q th) of their several objective functions (fitness functions). This provides a sequence, and, thus, defines the nearest neighbors of any chromosome in front j

b) Find the largest cuboid (rectangle for two fitness functions) enclosing chromosome i that just touches its nearest neighbors in the f-space

c) $I_{i,dist}$ = 1/2× (sum of all sides of this cuboid)

d) Assign large values of $I_{i,dist}$ to solutions at the boundaries (the convergence characteristics would be influenced by this choice)

(4) Make N_p copies randomly (duplication permissible), of the better chromosomes from P' into a new box, P" using:

a) Select any pair, i and j, from P' (randomly, irrespective of fronts)

b) Identify the better of these two chromosomes. Chromosome i is better than chromosome j if:

$I_{i,rank} \neq I_{j,rank}$: $I_{i,rank} < I_{j,rank}$

$I_{i,rank} = I_{j,rank}$: $I_{i,dist} > I_{j,dist}$

c) Copy (without removing from P?) the better of these two chromosomes in a new box, P"

d) Repeat till P" has N_p members. Not all of P' need be in P". By this method, the better members of P' are copied into P" stochastically

(5) Copy all of P" in a new box, D, of size N_p. Carry out crossover (using the stochastic remainder roulette-wheel selection procedure, **Deb, 1995**) and mutation (**Deb, 1995**) of chromosomes in D. This gives a box of N_p daughter chromosomes.

(6) JG Operation: Select a chromosome (sequentially) from D. Check if JG operation is needed, using P_{jump}. If yes:

a) Generate a random number (between 0 and 1)

b) Multiply this by lchr, the total number of binaries in the chromosome. Round-off to convert into an integer. This represents the position of one end (either beginning or end) of a transposon

c) Repeat steps 6a and 6b to identify the second end of the transposon

d) Invert or replace the set of binaries between these locations (use random numbers to generate the transposon for the case of replacement)

(7) Elitism: Copy all the N_p best parents (P") and all the N_p daughters with transposons (D) into box PD. Box PD has $2N_p$ chromosomes

a) Reclassify these $2N_p$ chromosomes into fronts (box PD') using only non-domination (as described in Step 2 above)

b) Take the best N_p from box PD' and put into box P"

(8) This completes one generation. Stop if appropriate criteria are met, e.g., the generation number › maximum number of generations (user specified).

(9) Copy P"" into starting box, P. Go to Step 2 above.

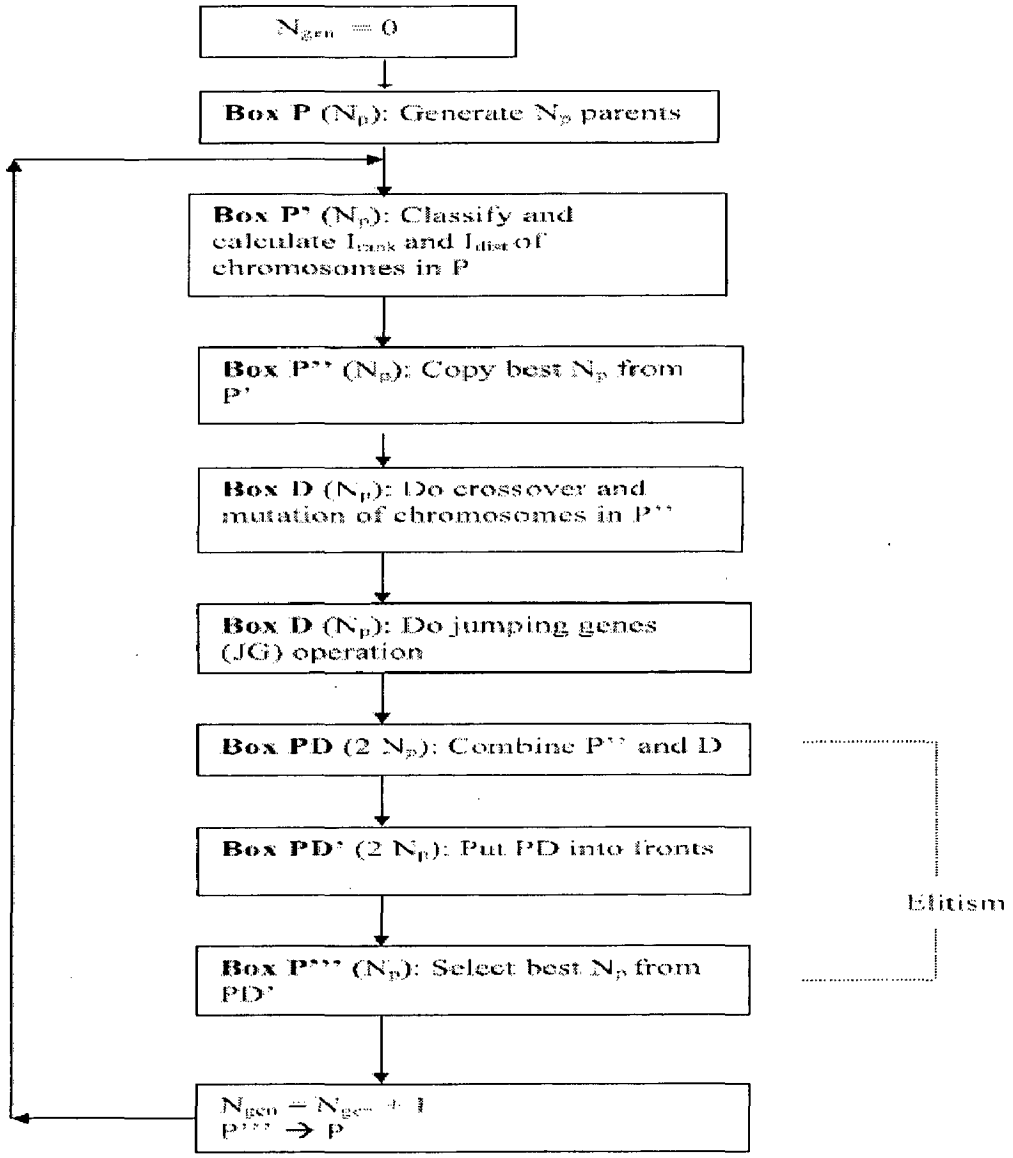

Figure A2: Flowchart of NSGA-II-JG.